A STUDY OF AXIAL TURBINE LOSS MODELS IN A STREAMLINE CURVATURE COMPUTING SCHEME

by

SATISH KUMAR

DEPARTMENT OF AERONAUTICAL ENGINEERING
INDIAN INSTITUTE OF TECHNOLOGY KANPUR
SEPTEMBER, 1982

A STUDY OF AXIAL TURBINE LOSS MODELS IN A STREAMLINE CURVATURE COMPUTING SCHEME

A Thesis Submitted
In Partial Fulfilment of the Requirements
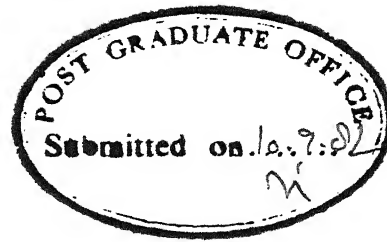for the Degree of
MASTER OF TECHNOLOGY

by

SATISH KUMAR

to the
DEPARTMENT OF AERONAUTICAL ENGINEERING
INDIAN INSTITUTE OF TECHNOLOGY KANPUR
SEPTEMBER, 1982

CERTIFICATE

This is to certify that the thesis entitled
"A Study of Axial Turbine Loss Models in a Streamline
Curvature Computing Scheme" by Satish Kumar is a
record of work carried out under my supervision
and has not been submitted elsewhere for a degree.

Dr. R.K. Sullerey
Asst. Prof., Dept. of Aeronautical Engg.
I.I.T., Kanpur.

Dated : 6th September, 1982.

ACKNOWLEDGEMENTS

TABLE OF CONTENTS

ABSTRACT

The present investigations study the applications
of various loss models for axial turbines in a streamline
curvature method calculating scheme. Among the loss correlat
used are the recently modified form of Ainley-Mathieson and
Dunham-Came loss correlation, Balje-Binsley correlation
and its modification and a loss correlation based on Soder-
bergs loss model. Extensive analysis has been carried out
for the cases of single stage, three stage and four stage
turbines including off-design calculations. The computed
results have been compared with the available experimental
data for these turbines. The results indicate that the
modified Ainley-Mathieson and Dunham-Came loss model gives
accurate prediction of various parameters including effici-
encies. Balje-Binsley loss correlation appears to be equally
good if its secondary loss correlation is replaced by more
realistic Dunham-Came loss model.

NOMENCLATURE

Abreviation	Description
AMDC	Ainley-Mathieson and Dunham-Came
BBDC	Balje-Binsley and Dunham-Came

Symbol	Description
b_c	Blade Chord
b_h	Blade Height
b_s	Blade Specing
b_t	Blade Thickness
c_p	Specific Heat at constant pressure
cr	Rotor Blade chord
D	Diameter at tip of rotor
h	Enthalpy
H	Boundary layer form facter
j	Streamline index
K	Mach number correction factor for profile loss coefficient
l	Blade camber line length
M	Mach number
m	Meriodional coordinate
P	Non dimensional power function
p	Static pressure
p_o	Stagnation pressure
R	Gas constant
r	Radius
r_m	Streamline radius of curvature.

Symbol	Description
S	Entropy
s	Blade tip clearance
T	Static temperature
T_o	Total temperature
t	Time
t_e	Blade trailing edge thickness
u	Blade speed
V	Velocity
$\overline{W}$	Work done
W	Relative velocity
w	Mass flow
x	Axial coordinate
Y	Pressure loss coefficient
ζ_P	Profile loss cofficient
ζ_e	End wall loss coefficient
ζ_{CL}	Tip clearance loss coefficient
β	Flow angle
γ	Specific heat ratio
δ	Deflection
δ_1	Initial boundary layer thickness
δ^*	Dimensionless displacement thickness
η_R	Rotor isentropic efficiency
η_S	Stage isentropic efficiency
ρ	Density
ω	Angular velocity
μ	Mixing coefficient

Symbol	Description
ϕ	Streamline slope
θ	Tangential coordinate
θ^*	Dimensionless momentum thickness
ν	Kinematic viscosity

Subscript	Description
AR	Aspect ratio
ex	Exit
h	Hub
in	Inlet
m	Meriodional component
N	Stator/Nozzle
R	Rotor
r	Radial component
T	Total
u	Tangential component
uR	Tangential component for rotor
x	Axial component

LIST OF FIGURES

CHAPTER - 1

INTRODUCTION :-

All those devices in which energy is transferred either
or from, a continuously flowing fluid by the dynamic action
of one or more moving blade rows are classified as turbomachine.
There are/main catagories of turbomachines :
i) those which absorb the power to increase the fluid pressure,
(compressors,pumps)ii)those that produce the power by expanding
the fluid to a lower pressure (turbines). Turbines are further
classified according to the nature of the flow path through
the passage of the rotor. When the path of the through flow
is wholly or mainly in a plane perpendicular to the rotation
axis in a turbine, then it is called a radial flow turbine, and
when the path of the through flow is wholly or mainly parallel
to the rotational axis,it is termed an axial flow turbine.
When both the radial and axial velocity components are present
in significant amount,the turbine is called mixed flow
turbine. Only axial flow turbines are used for aircraft
propulsion.

In order to predict the performance of a turbomachine,
we have to analyse the flow in it. The internal flow in
turbomachine in general is nonsteady, three dimensional and
viscous. Due to the extreme complexity of flow, the velocity
distribution through-out the flow field can-not be calculated

taking account of all these factors simultaneously. The design of the turbine consists of three major steps, the first is the determination of the requirement of the flow, work and speed. The second step is the evolution of the velocity diagram which should be consistent with the desired efficiency and number of stages. The third step is the design of the blading that will provide the necessary flow angles and velocities required by the velocity diagrams.

In early days majority of axial turbines used to be designed by using rather simple approach in which the flow at each of the design station was assumed to have :

(1) Radially constant values of total temperature and total pressure.

(2) Radial component of velocity are zero.

By using these assumptions the radial equilibrium equation is considerable simplified. One of the solution of the simple radial equilibrium equation is the free vortex solution in which the axial component of velocity is constant and tangential component varies inversly with the radius. The principal disadvantages of free vortex approach to the turbine design are that :

(1) Design method is very restrictive.

(2) Model is basically inaccurate, turbine test results clearly show the significant variation in axial velocity, total pressure and total temperature. So it is unrealistic

to assume that there would not be significant radial variations of total temperature and total pressure.

Since the advent of modern computers, more effective methods for solving radial equilibrium equation retaining the radial variation terms have come into vogue. The three dimensional flow problem is usually simplified by first solving the flow problem in various 2-D surfaces i.e. flow solution on mean hub to shroud stream surface which is commonly called a meridional surface, the other surfaces being blade to blade surface and orthognal surfaces. The blade to blade flow solution yields the blade surface velocity distribution. The following are the recent methods to solve the flow problem in blade to blade flow, some of which are equally suited to meridional flow solution.

(1) STREAM LINE CURVATURE METHOD :-

The stream line curvature method is also called as the stream filament method. This is a numerical method for solving the fluid dynamic problem. The basic model used for stream filament analysis of a turbine design consist of a series of streamlines which trace the path of the flow from known condition to the first stage and then to the final design station at the exit from the last blade row. Assuming that flow is axisymmetric through out the entire turbine, a series of the streamlines can be selected at turbine inlet to define a series of annular stream tubes. The position of the streamline is defined so that the adjacent stream surface

contains a known fraction of total flow. Since the flow is assumed axisymmetric, the flow through the turbine can be represented by a meriodional section as shown in fig. (1) .

However for, an analysis of geometry and design point performance of turbine, the main objective is to define the blading requirement also. Turbine is subdivided into a number of elements. These individual elements can not be considered in isolation for these are inter related by consideration of radial equilibrium and overall design requirements which include satisfying continuity equation at each of the design station. Hence the principal requirement for the stream filament analysis of a turbine design is the solution of radial equilibrium equation. This equation must take into account the radial variation of entropy & enthalpy.

In the meridional plane the flow equation may be written in the form of a gradient of meridional velocity, with radius. However, there are some additional terms associated with radial gradient in stagnation enthalpy and entropy, arising from work transfer and losses within the blade row. Additional parabolic equations for the change of these properties along the meridional stream line must be satisfied. The streamline curvature method of solution is used to solve this equation for velocity iteratively. The method is applicable to transonic flow as long as the Mach number based on meridional velocity is not close to unity.

(2) TIME MARCHING TECHNIQUE :-

There are several difficulties in implementing the streamline curvature and the matrix method in the supersonic & transonic regimes.

In the time marching technique the form of the equation is same throughout the flow field whether the flow is subsonic, supersonic or transonic in nature. The basic principle of time marching technique is to start with a guessed flow distribution and integrate the time dependent equation of motion and energy forward with time until a steady solution is obtained. It is possible to take care of the presence of shock waves by such techniques as shock fitting and shock capture.

(3) MATRIX METHOD :-

The matrix through flow method is so called because it calculates the flow within or through the blade row. The technique involves covering the region of interest with a fixed regular grid (as shown in Fig. (5A) and writing a finite difference approximation at every interior grid pt.

$$\frac{\partial^2 \psi}{\partial x^2} + \frac{\partial^2 \psi}{\partial y^2} = q \left(xy, \frac{\partial x}{\partial x}, \frac{\partial \psi}{\partial y} \right) \qquad (1.1)$$

This will results in one algebraic equation for every grid point in terms of stream function at that and

neighbouring point. The system of equations can be expressed in matrix form as

$$[A]\,[\Psi] = [Q] \qquad\qquad (1.2).$$

where $[A]$ is coefficient matrix derived from replacing the differential operator $\nabla^2 (\quad)$, $[\Psi]$ is the vector of unknown stream function value, and $[Q]$ is the vector of quantities $q(x,y)$ from equation (1.1).

Since the R.H.S. of equation (1.1) is a function of Ψ and its derivative, the system of equation is nonlinear and must be solved iteratively i.e., by first estimating $[\Psi]$, computing $[Q]$, and then repeatedly solving the equation (1.1) for $[\Psi]$. The value for $[Q]$ is improved/each iteration in using the previous value of $[\Psi]$.

Since A is the function of grid shape only, it need be computed and inverted only once. This is done by factoring $[A]$, which is a square matrix, into triangular matrics $[L]$ and (U). They can then be used for successive iteration and different boundary coditions. This method offers fast convergence, and **stability** at high flow rate and machine speed.

(4) <u>FINITE ELEMENT METHOD</u> :-

This method is very much similar to the matrix method. The main difference is that instead of using finite differencing

technique as in the matrix method, the finite element method is used in solving the governing equations. This method is comparatively new and in the process of development. Hirsch & Warzee (28) have described this method in much details.

LOSS MODEL :-

The losses arise in a turbine are due to the viscosity, Three dimensional effect (secondary flow, tip clearance) and mixing (interfilament mixing). These losses are called as the profile losses and the secondary losses. Analytical calculation of profile losses is difficult. In a real machine this loss can-not be isolated from other sources of loss, so prediction of profile loss are generally based on and compared with test made in cascade wind tunnel. There are two methods for prediction of the profile loss.

(1) This requires only simple blading parameter such as flow angle, pitch chord ratio, Reynolds number and Mach Number. This method is called the correlation method.

(2) A second method has been made possible by the advent of the digital computer. The loss is obtained from the calculation of velocity distribution and boundary layer growth on the blade surface. This method is called as calculation method.

The correlation method is necessary when deciding upon optimum stage geometry of the turbine design and would

usually be used in predicting the machine efficiency. The
calculation method can be used in place of cascade test when
optimizing the blade profile. In many situations this method
can not be used, e.g. when detailed blade profile is not
known or because of the time required in data prepration would
be more. The objective of various loss definition methods is
to provide for a loss in total pressure as normalized by some
suitable normalizing procedure which correlates well with
the experimental evidence. The basic purpose of the loss
model can be described in other way also, the equation of
flow used in the meridional flow analysis are written for an
inviscid flow. The analysis of the inviscid flow would be
of little importance in the prediction of performance of
turbine unless some method is found to take into account
change in entropy due to viscosity. This is done by using a
loss model. The loss model superposes on the inviscid flow the
changes in entropy (Effect of viscosity) by means of a/equation
^{loss}
(in the form of stagnation pressure loss or entropy change
or loss in kinetic energy).

It is evident that sophisticated numerical analysis
of a selected turbine design requirement would be of little
value if the blade row performance data used in conjuction
with the analysis were not consistent with the blading to be
used for design. The evaluation of losses in flow is achieved
from correlation of experimental data. A large amount of such

data is available in case of axial compressors. A NASA special
publication (NASA SP-36) on axial compressor has a collection
of such data. Mazumdar (36) has reviewed the different
correlation for axial compressor. Such a review or collection
of data is not available in a single source for the case of
axial turbines. There are several loss correlation available
in literature however, Some of these are rather old and may
not be particularly suited for modern blade technology.

Some of the well known loss correlations for the prediction
of the performance of axial flow turbines are, efficiency
correlation of Smith (26), Soderberg's loss correlation (22)
and Ainley Mathieson loss correlation (23). The secondary
loss correlation of Ainley Mathieson (23) was modified by
Dunham & Came (24). Another important correlation for
evaluating the losses is given by Balje and Binsley (27) based
on Zweifel's criterion for blade loading and Truckenbrodts
relation for momentum thickness.

REVIEW OF LITERATURE :-

Internal flow in turbomachine is extremely complex, in
general it is three dimensional, viscous and unsteady. The
most successful approach to the problem has been to solve the
flow in two families of intersecting surfaces, Blade to blade
surfaces and meriodional surface. In the analysis of blade
to blade plane problem, the flow relative to blade is
assumed to be steady and irrotational. Such solution are

then used in calculating the profiles losses using calculation methods. Solutions obtained by conformal transformation for incompressible flow are given for example by Merchant & COLLAR (1) and GOST ELOW (2) but this method is limited to the simple cascade geometries. The singularity method, in which blades are replaced by vortex and sink-source distributions has been used by SCHLICTING and SCHOLZ (37), ISAY and MARTENSEN (3) and WILKINSON (4) for incompressible flows. The singularity method has been extended for the subsonic compressible flow taking into care of compressibility corrections such as by VON KARMAN (5) and TSIEN (6).

A scheme for solution of compressible steady flow in the blade to blade plane was given by THEODORE KATSANIS (7). This method is basically applicable to subsonic flow but can
                    locally
also deal with/supersonic flows. The blades my be fixed or rotating. The flow may be axial, radial or mixed. This is one of the first applications of streamline curvature (velocity gradientmethod) technique. Subsequently the streamline curvature method used by Bindon & CARMICHAEL (8) in which a differential equation for the velocity gradient along the normal to the streamline is written in terms of the radius of curvature of streamline. This equation is integrated across the blade passage to give the velocity profile and constant of integration is determined by the continuity equation.   WILKINSON (9) used the same technique

but the main difference was that, they used the velocity gradient equation along the quasi-orthognal to the streamline, Further the same equation is written in terms of the stream function satisfying the continuity equation, given by SMITH & KATSANIS (10).

Recent development in calculation of the flows in the blade to blade plane includes the time marching technique. The difficulty of mixed, elliptic and hyperbolic domain has been overcome by use of time marching techniques, treating the governing time dependent equation for compressible flow. These equations were solved by Marsh and Merryweather (11) in the finite difference form using a Taylor series exapnasion around the grid point. Daneshyar and Glynn (12) have developed a more efficient time marching scheme based on the method of characterstic which shows comparable accuracy with that of MARSH & MERRY weather, neither of these scheme resort to the introduction of stabilizing device. GOPALAKRISHNAN & BOZZOLA (13) gave an introduction of such stablizing device. The foregoing methods do not give any explanation concerning shock location or entropy rise. Many flows however, contain only weak shocks which may be treated using the isentropic relation. MCDONALD (14) has shown good agreement between isentropic time marching theory and experiment for pressure distribution in which the maximum local Mach Number is around 1.43. This method is termed a finite area method. In an

application of finite element technique, AK-Y & ECER (15)
have analysed of the transonic flow through a cascade of
airfoils using the finite element method. This method consist
of the development of a computational grid suitable for
complex flow strcture and different boundary conditions have
been discussed. Modeling of the shock and the convergence
characterstic of the developed scheme has also been discussed.
Further the finite element technique for steady compressible
flow with the possible extension to unsteady flow is given
by THOMPSON (16).

In the meriodional plane the flow equation may be
written in the form of the gradient of meriodional velocity
along the radius. SMITH(17) has derived the exact radial
equilibrium equation in a form suitable for the stream line
curvature method. The equation has been derived by circum-
ferential averaging of the flow variables in the momentum
equation. NOVAK (18) has described in details the process
of solving the meriodional flow problem using the streamline
curvature method. He has derived the governing radial equilibrium
equation from the radial momentum equation of an inviscid flow
by making the use of axysmmetric assumption. NOVAK (18)
has also discussed the problem of an non-axisymmetric
computation which is necessary when computations are to be
made within a blade row where the axysymmetry assumption is
not valid. In a more sophisticated analysis, NOVAK & HEARSEY
(19) have obtained a "nearly three dimensional" solution to the

flow in a turbomachine by using the streamline curvature method and iterating between the solutions obtained on the blade to blade and meriodional planes. FROST (20) has also given a method so as to be able to make the computations within blade row. This has been achieved by using the concept of a "mean stream surface" developed for matrix method. The flow equations have been derived on this stream surface and the blade forces determined as that required to keep the flow in the surface. FROST (20) has called this method the 'Stream line curvature through flow method'. In an application to the gas turbine design, CARTER, PLATT and LENHERR (21) have used the streamline curvature method for the evaluation of the design point performance of axial turbine. The radial equilibrium equation has been simplified by neglecting the term involving the change in momentum in the meriodional direction by assuming that streamlines slope are small.

There are several loss correlations available in the literature. They are the SODERBERG LOSS CORRELATION (22). Soderberg has correlated the losses on a basis of space, chord ratio, Reynolds number, Aspect ratio, thickness ratio and blade geometry. AINLEY & MATHIESON (23) also correlates the profile drag at zero incidence and shows the profile drag for nozzle and impulse blading at various values of outlet angle and various space-chord ratio. DUNHAM & CAME (24)

gave their correlation for the secondary losses. KACKER &
OKAPUU (25) described a mean line loss system capable of
predicting the design point efficiency of current axial
turbines. They modified the secondary loss calculation given
by AINLEY/MATHIESON & DUNHA^M/CAME (24). They describe
the dependence of the secondary losses on the blade aspect
ratio. It is assumed that secondary losses varies as
reciprocal of blade aspect ratio, over the complete range of
aspect ratio. A modification to Soderberg's loss correlation
was developed by CARTER et. al. (21). They have made use
of Smith's efficiency correlation (26) in making this
modification. BALJI & BINSLEY (27) derived a generalized
loss correlation for turbines. The effects included were
Reynolds number, blade angle, blade height, number of blades,
trailing edge thickness, tip clearance and degree of reaction.

SCOPE OF PRESENT INVESTIGATION :-

In the present work a comparitive study of axial
turbine loss-models in a stream line curvature computing scheme
has been done. Earlier Govindan (39) had used the AMDC loss-
correlation, however it over predicted the losses. The modified
form of this model has recently been given by Kacker and
Okapuu (25), in which several correction factors have been
introduced in the profile and secondary loss correlations
and the level of profile loss has also been reduced. In
addition Balje Binsley loss model, and its modification have
also been used. Comparision of the loss models have been

done on the basis of design pressure ratio as well as based on the design mass flow. The Carter's loss model has been used for single stage turbine, and for multistage turbine for a design pressure ratio.

Extensive computations have been carried out for three test turbines using these loss models. Computations have also been carried out for off -design case by varying the mass flow rate at the design r.p.m. The specific heat values have been specified according to the temperature values at the various design stations. A fifty percent value of mixing coefficient (for interfilament mixing) has been used. The use of mixing coefficient is essentially as a help in the convergence as its effect on computed results is insignificant. The results have been plotted using the Graphical Terminal of DEC - 10 computer.

CHAPTER - 2

FORMULATION & APPROACH TO SOLUTION

2.1 FORMULATION :-

Three dimensional inviscid pattern of flow can be solved by using the following equations :-

1. Equation of motion

2. Energy equation

3. Continuity equation

4. Equation of state.

By solving these equation we can determine the fluid properties like, density enthalpy entropy and the three component of velocity. If we combine the three equations of motion with energy equation, we can obtain an equation for reversible adiabatic flow which states that entropy of fluid remains constant along any stream line. If a reversible adiabatic flow takes place on a prescribed stream surface, then there exists a geometrical condition relating to the three components of velocity vector in order that the velocity vector lies on the stream surface. The flow pattern is obtained by replacing one of the equation of motion with the geometrical condition for the flow to remain on the stream surface. The replaced equation of motion can be used to evaluate the force necessary to keep the flow on the stream surface. This force, for an inviscid flow, lies normal to the surface and is

contained only in the equation of motion for this direction. Thus for an reversible adiabatic flow on a prescribed stream surface the flow pattern can be determined by the following equations:-

(1) Continuity

(2)(a) Any two of : x equation of motion

r equation of motion .

s entropy

(b) Geometrical condition

(3) Energy

(4) State

For an irreversible adiabatic flow, the entropy increases along the streamlines and this effect is taken into account by means of the loss model. Since the irreversibility of flow is caused by the viscous effects. The introduction of a loss model superposes the viscous effects of the real flow on an otherwise inviscid formulation.

The following one the set of equations that are widely used in the analysis of the flow in turbomachine and has been used in the present investigations.

(1) Continuity

(2)(a) Equation of motions (r direction) or (Radial equilibrium equation)

(b) entropy (loss model)

(c) Geometrical condition

(3) energy equation

(4) equation of state

2.2 DISCRIPTION OF EQUATIONS :-

The following assumption have been made in the derivation of radial equilibrium equation :-

(1) Fluid is frictionless

(2) The Rotor is rigid and rotates with constant angular velocity

(3) Flow is steady and axysymmetric

(4) The fluid is a semi perfect gas i.e. the equation of state is $P = \rho RT$ (2.1) with R constant & the specific heat are dependent only upon the temperature.

For a frame of reference rotating with constant angular velocity ω about the z axis, Newtons 2nd law of motion gives for frictionless fluid.

$$-\frac{\nabla P}{\rho} = \frac{D\vec{W}}{Dt} - \omega^2 \vec{r} + 2\vec{\omega} \times \vec{W} \qquad 2.2$$

It is convenient to use the relative cylinderical coordinate system, r, θ & z, The unit vector derivatives are

$$\frac{D\vec{I_r}}{Dt} = \frac{W_u}{r} \vec{I_u} \quad \& \quad \frac{D\vec{I_u}}{Dt} = -\frac{W_u \vec{I_r}}{r}$$

and the kinematic relation $\dfrac{D(\quad)}{Dt} = W \dfrac{D(\quad)}{Ds}$

The capital D operator signifies that a fluid particle is being followed during the differentiation. The quation (2.2)

can be written in terms of its scalar components are

$$-\frac{1}{\rho}\ \frac{\partial P}{\partial r} = W\ \frac{DW_r}{Ds} - \left(\frac{W_u + \omega r)^2}{r}\right) \qquad \underline{\qquad} (2.3a)$$

$$-\frac{1}{\rho}\ \frac{P}{r\partial \theta} = W\ \frac{DW_u}{Ds} + \frac{W_u\,W_r}{r} + 2\,\omega\,W_r \quad \underline{\qquad}(2.3b)$$

$$-\frac{1}{\rho}\ \frac{\partial P}{\partial x} = W\ \frac{DW_x}{Ds} \qquad \underline{\qquad} (2.3c)$$

By the use of the substitution $V_u = W_u + \omega r$, between the absolute & relative velocities, the equation no. (2.3a) & (2.3b) can be written as

$$-\frac{1}{\rho}\ \frac{\partial P}{\partial r} = W\ \frac{DW_r}{DS} - \frac{V_u^2}{r} \qquad \underline{\qquad} (2.4a)$$

$$-\frac{1}{\rho}\ \frac{\partial P}{r\partial \theta} = \frac{W}{r}\ \frac{D}{DS}(r\,V_u) \qquad \underline{\qquad} (2.4b)$$

we can also write

$$W\ \frac{D(\quad)}{ds} = W_x\ \frac{D(\quad)}{Dx} \qquad \underline{\qquad} (2.5)$$

Where Dx represent increase in the x coordinate the particle undergoes as it moves a distance DS in the flow direction. Equation like (2.5) can be written for any desired direction. A direction of particular interest here is the meriodional direction defined by

$$\vec{I}_m\,D_m = \vec{I}_x\,D_x + \vec{I}_r\,D_r \qquad \underline{\qquad} (2.6)$$

Equation (2.5) becomes as

$$W \frac{D \; (\quad)}{DS} = W_m \frac{D \; (\quad)}{Dm} \qquad \underline{\qquad\qquad} (2.7)$$

Substituting equation (2.7) in equation no. (2.4a), we get

$$-\frac{1}{\varsigma} \frac{\partial P}{\partial r} = W_m \frac{D \; W_r}{D_m} - \frac{V_u^2}{r} \qquad \underline{\qquad\qquad} (2.8)$$

Further we can write $W_r = W_m \sin \emptyset$ $\underline{\qquad\qquad}$ (2.9)

Equation (2.8) can be rewritten as

$$\frac{1}{\varsigma} \frac{\partial P}{\partial r} = \frac{V_u^2}{r} - w_m^2 \frac{D \sin \phi}{D_m} - W_m \sin \phi \frac{D \; W_m}{D_m} \underline{\qquad} (2.10)$$

Now $\qquad \dfrac{D \sin \phi}{D_m} = \cos \phi \dfrac{D \phi}{D_m}$ $\qquad\qquad$ (2.11)

and $\qquad \dfrac{D \psi}{D_m} = -\dfrac{1}{r_m}$

The radius of curvature is choosed negative when the streamline projection on the meriodional plane is concave upwards

Now the equation (2.10) can be rewritten again

$$\frac{1}{\varsigma} \frac{\partial P}{\partial r} = \frac{V_u^2}{r} + \cos \phi \frac{w_m^2}{r_m} - W_r \frac{DW_m}{D_m} \qquad \underline{\qquad}(2.12)$$

in terms of the absolute velocity components, equation (2.12) becomes as

$$\frac{1}{\varsigma} \frac{\partial P}{\partial r} = \frac{V_u^2}{r} + \cos \phi \frac{V_m^2}{r_m} - V_m \sin \phi \frac{D \; V_m}{D_m} \qquad \underline{\qquad} (2.13)$$

Equation (2.13) is written in a more convenient forms by

replacing the static pressure by the stagnation pressure from

$$P = P_o \left[1 - \frac{V_u^2 + V_m^2}{2C_p \, To} \right]^{\frac{\gamma}{\gamma-1}}$$

we get

$$\frac{V_u^2 + V_m^2}{2} \quad \frac{1}{To} \quad \frac{dTo}{dr} - V_u \frac{DV_u}{dr} - \tfrac{1}{2} \frac{dV_m^2}{dr} + RTo \left[1 - \frac{V_u^2 + V_m^2}{2C_p \, To} \right]$$

$$\frac{1}{Po} \frac{dPo}{dr} = \frac{V_u^2}{r} + \frac{V_m^2 \, Cos\phi}{r_m} - V_m \, Sin\phi \, \frac{DV_m}{D_m} \quad \text{_____} \quad (2.14)$$

Again it is necessary to express the terms $\dfrac{DV_m}{D_m}$ in terms

of the meriodional path line slope & curvature. By making

the use of continuity equation, equation of state, laws

of thermodynamics, it can be shown in (Appendix A).

$$Sin\phi \, \frac{DV_m}{D_m} = \frac{\left[V_m \, (1+M_e^2 \, + 1 \, \frac{r}{r_m} \, cos\phi) \, \frac{Sin^2\phi}{r} + tan\phi \, \frac{\partial\phi}{\partial r} \right]}{1 - M_m^2} \quad (2.15)$$

2.2.2 CONTINUITY EQUATION :-

The continuity equation provides the necessary condition

for the determination of constant of integration when integrating

the radial equilibrium equation. The location of the stream-

lines at each of the design station and meriodional velocity

at each of the streamlines are determined from the mass

flow continuity equation. For an axysymmetric flow passing

through an axial section of an arbitrary annulus, the continuity equation is as follows :

$$W_T = 2\pi \int_{r_h}^{r_c} V_x \, \rho \, r \, dr \qquad \underline{\qquad}(2.16)$$

where W_T is total mass flow in kg./sec., ρ is the static density in kg/m^3 r_h & r_c are hub and casing radii of the sections.

Reformulating the equation no. (2.16) in terms of Total Temperature, Total pressure, Tangential & meriodional components of velocity. Substituting for the density in (2.16).

$$\rho = \frac{Po}{RTo} \left[1 - \frac{V^2}{2 C_p T_o}\right]^{\frac{1}{\gamma-1}} \qquad \underline{\qquad}(2.17)$$

The equation no. (1.16) can be expressed as follows

$$W_T = \frac{2\pi}{R} \int_{r_h}^{r_c} \frac{Po}{To} \left[1 - \frac{V_u^2 + V_m^2}{2 C_p T_o}\right]^{\frac{1}{\gamma-1}} V_m \cos\phi \, r \, dr \underline{\qquad}(2.18)$$

Since the radius dependent variable of above equation will not be simple analytical function of radius, the distribution of meriodional velocity which satisfy the continuity equation will have to be obtained using an iterative numerical procedure.

2.2.3 THE LOSS EQUATION :-

Since the total temperature & total pressure are choosen as the principal variable in the analysis, the

irreversibility of flow is more conveniently expressed in terms of stagnation pressure loss. The total pressure loss coefficient is defined as follow :

$$Y_N = \frac{P_{o0} - P_{o_1}}{P_{o_1} - P_1} \qquad \underline{\qquad} (2.19)$$

$$\text{or} \qquad P_{o_1} = \frac{P_{o0}}{1 + Y_N \left(1 - \frac{P_1}{P_{o_1}}\right)} \qquad \underline{\qquad} (2.20)$$

For the rotor, loss coefficient is defined as

$$Y_R = \frac{P'_{o_2S} - P'_{o_2}}{P'_{o_2} - P_2} \qquad \underline{\qquad} (\,2.21)$$

$$\text{or} \qquad P'_{o_2} = \frac{P'_{o_{2s}}}{1 + Y_R \left(\frac{1 - P_2}{P'_{o_2}}\right)} \qquad \underline{\qquad} (2.22)$$

The above relations are used to determine the stagnation pressure loss when the total pressure loss coefficients are known from the loss correlation of experimental loss data in the form of a loss model.

2.2.5 THE WORK EQUATION :-

The total temperature will be obtained from the specified work which is readily expressed in terms of the total temperature, drop. Thus

$$C_p \Delta T_o = \overline{W} \qquad \underline{\qquad} (2.25)$$

w is the work extracted along the streamline the tangential velocity component is obtained using the Euler work equation as

$$C_p \triangle To = V_{u1} u_1 - V_{u2} u_2 \qquad \underline{\quad} (2.26)$$

or

$$V_{u2} = \frac{V_{u1} u_1 - C_p \triangle To}{u_2} \qquad \underline{\quad} (2.27)$$

The equation is used in analysis when design work is specified.

2.2.6 GEOMETRICAL CONDITION :-

At a stater exit the tangential velocity is related to the meriodional velocity from a specification of exit flow angle in velocity triangle. i.e.

$$V_u = V_m \cos \phi \tan \beta \qquad \underline{\quad} (2.28)$$

2.2.7

Denton (30) also described stream line curvature method for through flow calculation for transonic axial flow turbines. From the assumption of axial symmetry it is possible to define a series of meriodional stream surface. There are surface of revolution along which the fluid particle are assumed to move through the machine. The principle of stream line curvature is to write the equation of motion along the lines roughly perpendicular to these stream surface (i.e. along quasi-orthogonal lines) in terms of the curvature of the

surface in the meriodional plane. Quasi-orthogonal is a
fixed line which goes from one wall to theother of the channel
confining the flow, all of the mass flow therefore crosses it
and this is used to satisfy the continuity equation by
adjusting the velocity level along the quasi-orthogonal to
give the correct mass flow.

2.3 APPROACH TO THE SOLUTION OF THE EQUATION :-

The solution of the flow field in case of the axial
turbine essentially consists of obtaining values of total
temperature, total pressure, and two components of the absolute
velocity (V_u and V_m) i.e. Po, To, V_u and V_m are the principal
variables. For the solution we have the sets of equations in
terms of these variables. The set of equations, for the
solution, would comprise of equation (2.14). The appropriate
equation in the set of equation (2.19) to (2.22) and equation
(2.25) to (2.28.)

It is obvious that the principal equation is the
Radial equilibrium equation (2.19). This is an ordinary
differential equation, nonlinear in variable V_m. The rest
of the equations will be used for the evaluation of the other
flow variables in equation (2.14). However the streamline
solope and curvature in the meriodional plane, ϕ and $1/r_m$,
still necessitate consideration of derivatives with respect
to the axial direction, x. i.e.

$$\phi = \tan^{-1} \left(\frac{dr}{dx} \right) \qquad \underline{\qquad} \quad (2.29)$$

and

$$\frac{1}{r_m} = \frac{\dfrac{d^2 r}{dx^2}}{\left[1 + (dr/dx)^2 \right]^{3/2}} \qquad \underline{\qquad} \quad (2.30)$$

Hence the radial equilibrium equation contains the derivative w.r. to both r & x of the analysis were to be performed for an axisymmetric flow in an arbitrary duct, it could readily be extended to consider the path of individual streamline in the meriodional plane. However, in a turbine design point analysis, it is unrealistic to assume that axisymmetric form of the radial equilibrium equation can be extended beyond the interblade row space into the blade row. Thus, the boundary conditions for the meriodional streamlines in the interblade row space are indeterminate at the trailing edge and leading edge planes defining this space. Only the boundary streamlines, at the inner and outer annulus walls, are defined by the assumption that these streamlines follow the contours of annulus walls. In the meriodional plane for the slope and curvature of the flow, it becomes necessary to adopt an arbitrary solution to the problem. The streamline slope & curvature in the meriodional plane will be treated in one of the three ways

(a) The slope and curvature of boundary streamlines will be obtained from a definition of the wall contour, and then both ϕ and $1/r_m$ will be assumed to be linear function of radius determined from values at the wall.

(b) The slope and curvature will both be specified
    arbitrarily as a function of radius.

(c) The use of spline fitting technique.

The use of the spline fitting techniques for calculating
the streamline slope and curvature have been adopted by many
authors. Daneshywar, et. al. (38) have made a critical
assessment of this method for use in streamline curvature
technique. The instability which may occur in this technique
is due to the oscillation of the second derivative of the
spline curve which is used to calculate the streamline curvature.
To overcome this problem, DANESHYWAR et.al. (38) have
suggested the use of two spline curves, the first one fitted
to points through which the streamline passes, from which
the streamline slopes are calculated, the second one fitted
to the calculated slope at given axial stations and is used
to calculate the second derivative and hence the streamline
curvature.

DENTON (30) described one more method to obtain
stream surface slope and curvature on the basis of experience
with earlier programs. Which showed that overall accuracy
was determined more by the empirical inputs to the program
than by numerical scheme. It was decided to use a simple
parabolic curve fit to obtain stream surface slope and
curvature. The axis of parabola is chosen to be perpendicular to
the line of joining its outer two points so that calculation

can be continued round ducts with up to 180° turnings. The
parabola is a good means of obtaining the curvature being
more accurate than many more complex curve fits. In the present
analysis the spline fit technique has been used, which leads
to the solution of a diagonal matrix, which is easily done
on a computer.

A numerical solution of the radial equilibrium equation
is an iterative process. The continuity equation will provide
the boundary conditions for the evaluation of the constant
of integration in the radial equilibrium equation.

2.4 THE DIFFERENTIAL EQUATIONS :-

Since the radial equilibrium equation has to be solved
simeltaneously with two basic stream lines equations (The
tangential-momentum equation & total pressure loss equations).
The principal analysis variable considered are $\frac{dV^2_m}{dr}$, $\frac{1}{Po} \frac{dPo}{dr}$,
and $\frac{dV_u}{dr}$. Therefore radial equilibrium equation can be
written as

$$C_{11} \frac{dV^2_m}{dr} + C_{12} \frac{1}{Po} \frac{dPo}{dr} + C_{13} \frac{dV_u}{dr} = C_{14} \quad \_\_ \quad (2.31)$$

Where the coefficient C_{11}, C_{12}, C_{13} can be assigned
values at each point in a particular design plane once a
value of meriodional velocity is selected. The variables
To, ϕ , V_m and r and constants γ & C_p are assumed to have
been evaluated.

The differentiation of appropriate equation (2.20) or (2.22), (depending on the station and option being considered) leads to a differential equation of the form of

$$C_{21} \ \frac{dV_m^2}{dr} + C_{22} \ \frac{1}{Po} \ \frac{dPc}{dr} + C_{23} \ \frac{dV_u}{dr} = C_{24} \ \underline{\quad\quad} \ (2.32)$$

Where coefficient C_{21}, C_{22}, C_{23} & C_{24} can be evaluated in terms of input specifications and meriodional velocity.

Similarly differentiation of either of equation (2.27) or (2.28) for V_u result in a differential equation of the form of

$$C_{31} \ \frac{dV_m^2}{dr} + C_{32} \ \frac{1}{Po} \ \frac{dPo}{dr} + C_{33} \ \frac{dV_u}{dr} = C_{34} \ \underline{\quad\quad} (2.33)$$

In this case coefficient C_{32} is always zero. The terms involved in the coefficients are present in Appendix (C) after differention of appropriate equation.

2.5   TECHNIQUE FOR SOLUTION :-

The rewritting of the equations described above in the form (2.31), (2.32) and (2.33) helps in developing an unique technique for the solution irrespective of the design station being considerd, only the coefficient of differential equations differ from station to station. Now the problem is to obtain the meriodional velocity distribution which simeltuneously satisfy the radial equilibrium and continuity equation. By choosing the initial value of the meridional velocity at one streamline position, the local values of the coefficients of

the set of equations (2.31), (2.32), (2.33) can be obtained.
These equations are now solved for the derivative dv^2m/dr.
The value of meriodionalvelocity at any adjacent streamline
can be obtained by using the standard Runge-Kutta-Gill method
for solving the ordinary differential equation given in (Appendix-D)
Using the new value of the meriodional velocity values of total
pressure, tangential velocity and coefficients can be obtained
at the new streamline. Thus the derivative dV^2m/dr can be
obtained at this new streamline also. The process is repeated
until the meriodional velocity is obtained at each of the
streamlines used in the analysis. Using the continuity equation
the mass flow for the meriodional velocity distribution obtained
is evaluated. Since the solution was obtained from an assumed
value of meriodional velocity at one point in the flow field,
the mass flow computed will in general differ from disigned
specified value. Hence the assumed value of the meriodional
velocity will have to be modified iteratively until the
starting value is consistent with continuity requirement.
This constitute the inner loop of iteration procedure.

The evaluation of the streamline slope and curvature
constitute the outer loop of iteration and this can be evaluated
by one of the method as suggested above in the section (2.3)(a)
and (b). In the case of 2.3(a) the slope & curvature are
function of only radius at given design station. This can be
completed as follows : Since initially the flow distribution

unknown, the initial streamline position are estimated from
equal area for each stream tube. Hence, streamline positions
have to be relocated after each solution of the radial equili-
brium and continuity equation until a converged solution for
streamline position has been obtained. This completes the
solution at a design station and analysis can be proceed to
next design station downstream.

LOSS - MODELS

3.1. INTRODUCTION :-

The equation of flow used in the stream line curvature method, are for an invisicid flow. However, the analysis of the inviscid flow would be of little use in prediction of the performance of the turbine unless some method is found to take into account the change in entropy due to viscosity. This is the basic purpose of loss-model. Hence, an essential part of the development of a design analysis computing system is the development of a loss correlation which would be an integral part of the computer programme.

Loss data is limited in case of axial turbines as compared to the axial compressors. But there are few most commonly used correlations such as/Soderberg's Correlation and Ainley Mathieson loss correlation. These correlations have been developed using data obtained from the early gas turbines and steam turbines.

Four loss models have been used in this work. One of these have been developed by Carter et. al. (21).Second loss model has been proposed by Kacker and Okapuu (25) which is a modified form of AMDC (Ainley-Mathieson & Dunham-Came) loss correlation. The third loss model is due to Balje and Binsley (27) which has one of the best correlation for profile losses. Fourth loss model is a combination of Balje-Binsley (27)

and Dunham-Came (24) loss model in which the profile loss
is the same as in the Balje loss model but the secondary
losses have been introduced as given by Dunham and Came. All
these correlations have been discussed in this chapter.

3.2 DESCRIPTION OF LOSS MODELS

3.2.1. LOSS MODEL - 1 :-

The loss correlation was incorporated by Carter et.
al. (21) in their turbine design programme. In the analysis
of the blade element performance, total pressure loss
coefficient, kinetic energy loss coefficient or blade efficiency
are much useful in terms of which the row performance may
be expressed. Evidently such a model is only used when data
is available from experimental investigation. Use of such
model is restrictive to preliminary design analysis only.
Basically this loss model is the modification of the Soderberg
(22) loss model.

One of the widely used correlation (due to Soderberg)
assumes that loss is principally a function of deflection.
Hence one of the first correlation attempted was total
pressure loss coefficient verses deflection. Certain curves
were plotted.

points having the same exit angle were joined by a line and value of the row reaction were noted for each point. The data are correlated to a reasonable degree of accuracy by the following expression:

$$Y = (0.000.7\delta + 0.000005\ \delta^2)\ \{3-9\ (\frac{V_{in}}{V_{ex}}) + 10(\frac{V_{in}}{V_{ex}})^2\}\ (3.1)$$

The above correlation implies that when the velocity ratio $\frac{V_{in}}{V_{ex}}$, falls below .45, The level of the losses for a selected deflection begins to increase. This result is unacceptable, Since it is to be expected that losses will decrease smoothly as the overall row acceleration increase at constant deflection. The high reaction blading with low values of V_{in}/V_{ex} will have the high values of exit angles. Hence the possibility that increase in the loss was due to the trailing edge blockage effect. In order to avoid the above contradiction, Carter et. al (21) found that use of deflection as a correlating parameter is clearly the reason for theoretically unsound dependence on velocity ratio given in the equation (3.1).
So it is logical to consider tangents of/inlet & exit angles rather than the actual angles in the correlation. The selected correlation is of the form

$$Y = \frac{|\tan\beta_{in} - \tan\beta_{ex}|}{(a_4 + a_5\cos\beta_{ex})}\ \{a_1 + a_2(\frac{V_m}{V_{ex}} - a_3)\}$$

$$if\quad \frac{V_m}{V_{ex}} \geqslant a_3 \qquad\qquad (3.2)\{a)$$

$$Y = \frac{\left| \tan \beta_{in} - \tan \beta_{ex} \right|}{(a_4 + a_5 \cos \beta_{ex})} \left\{ a_6 + a_7 \left(\frac{V_{in}}{V_{ex}} \right)^{a_8} \right\}$$

$$\text{if} \quad \frac{V_m}{V_{ex}} < a_3 \qquad\qquad (3.2) \ (b)$$

Where a_1 to a_8 are the coefficients. The velocity ratio dependent on the function using $a_1 = 0.055$, $a_2 = 0.15$, $a_3 = 0.6$, $a_6 = 0.03$, $a_7 = 0.157255$, and $a_8 = 3.6$. The values of these constant/obtained from Smith correlation (26). This particular type of the correlation is Suitable for design analysis.

The loss model discussed above has some disadvantages which are given bas .elow :

(1) The use of this loss model is limited by the availability of data to use the pressure loss coefficient, Kinetic energy loss coefficient or blade efficiency as input to the calculation scheme.

(2) The development of this loss model shows that the row velocity ratio and the blade angles are the relevant parameters of the correlation. As an example., the blade angle at the hub of turbine is maximum and decrease towards the tip section of the blade. This is true for most of the turbine, so according to this correlation the losses will be maximum at the hub and minimum at the tip region. This is quite contradictory to the experimental evidences, experimentally it has been observed that the losses are

minimum in the central region of the annulus and increase towards the hub and tip region. So this correlation cannot correctly predict the distribution of these losses across the annulus and can predict only the overall efficiency and average losses.

3.3.2 KACKER AND OKAPUU LOSS MODEL :-

AMDC loss model has been replaced by the Kacker and Okapuu[25]Loss Model, because AMDC loss model over predicts the losses. To analyse the distribution of losses in the annulus of turbine, it is essential to divide the losses into the principal constituents, namely, the profile losses and the secondary losses.

A start is made using the two correlation for profile loss coefficient (Y_p) obtained from cascade data, which are for the nozzle type blade ($\beta_1 = 0$) and impulse type blade ($\beta_1 = \beta_2$) of conventional profile having the thickness chord ratio of 0.20. The profile losses are calculated in the Ainley mathieson model using the following correlation.

$$Y_p = \left[Y_p (\beta_1 = 0) + \left(\frac{\beta_1}{\beta_2} \right)^2 \left(Y_p (\beta_1 = \beta_2) - Y_p (\beta_1 = 0) \right) \right]$$

$$\left(\frac{b_t / b_c}{0.20} \right)^{\beta_1 / \beta_2} \tag{3.3a}$$

This correlation is primarily dependent on the blade angles, the secondary and tip clearance loss data have been correlated by using the concept of lift and drag coefficients and can be given as follows:-

$$Y_s + Y_c = (\lambda + B \frac{\tau}{H}) \left(\frac{C_L}{b_s/b_c}\right)^2 \frac{\cos^2 \beta_2}{\cos^3 \beta_m} \underline{\quad} (3.3.b)$$

More often used correlation for secondary losses been given by Dunham & Came (24) which is of the following form

$$Y_s = b_c/b_h (\cos \beta_2 / \cos \beta_1) (C_1/b_s/b_c)^2 \cos^2 \beta_2/\cos^3 \beta_m$$

$$\text{function } (\delta_1/b_c) \underline{\quad} (3.4)$$

where δ_1 is the inlet boundary layer thickness which is difficult to calculate. Therefore Dunham and Came (24) have replacing the function (of δ_1) by a constant. The value of constant has been taken as 0.0334.

$$Y_s = 0.0334 \left(\frac{b_c}{b_h}\right) \left(\frac{\cos \beta_2}{\cos \beta_1}\right) z \underline{\quad} (3.5)$$

where Z is the Ainley mathieson loading parameter.

$$Z = \left(\frac{C_1}{b_s/b_c}\right)^2 \frac{\cos^2 \beta_2}{\cos^3 \beta_m} \underline{\quad} (3.6)$$

The secondary loss was distributed across the annulus

$$Y_s (r) = A r^2 + B r + C \underline{\quad} (3.7)$$

A,B,C are constants, and can be evaluated by the
following three conditions :-

(1) The mass-averaged secondary loss obtained from (3.7) is
    that evaluated using the correlation (3.5)

(2) The secondary losses are zero at mean stream line.

(3) The slope of the distribution is zero at the mean
    streamline.

Thus the total loss at any stream line is

$$Y = Y_p + Y_s(r).$$

This **kind** of parabolic distribution of secondary losses
was used by Govindan (39). The loss model of Kacker and
Okapuu (25) is based on the previously mentioned AMDC corre-
lation. The profile losses, modified by Kacker & Okapuu (25)
has taken into account the effect of exit mach Number and
channel acceleration respectively. The combined effect of
these correlation is

$K_p = 1-K_2(1-K_1)$. Therefore the profile loss coefficient
Y_p given by AMDC (24) becomes as $Y_p = 0.918(\frac{2}{3} Y_{p,AMDC} K_p)$ ___(3.75)
where K_p, K_1 and K_2 can be calculated by the graphs given
by Kacker and Okapuu (25).

They gave the dependence of secondary loss calculation
on the blade aspect ratio. In the AMDC loss model it was
assumed that secondary losses varies as the reciprocal of
blade aspect ratio, over the complete range of aspect ratio.

Kacker et. al (25) noted that AMDC loss model predicted a more rapid increase in losses as the aspect ratio was reduced in the present loss system this rise in secondary loss (with a reduction in aspect ratio) is less rapid for aspect ratio less than two. They gave a loss model as

$$f(A.R) = \frac{1 - 0.25 \sqrt{2 b_h/b_c}}{b_h/b_c} \quad \text{for } b_h/b_c \leq 2 \qquad \underline{\hspace{1cm}} (3.76)$$

$$= \frac{1}{b_h/b_c} \quad \text{for } b_h/b_c > 2 \qquad \underline{\hspace{1cm}}$$

$$Y_s = 1.2 \ Y_s \ \text{AMDC} \ K_s \qquad \underline{\hspace{1cm}} (3.8)$$

where $K_s = 1 - K_3 (1 - K_p)$

and $K_p = 1 - K_2 (1 - K_1)$

The values of K_1 K_2 and K_3 can be calculated by the graphs given by Kacker and Okapuu (25). This loss-model gives the more satisfactory result than the A.M.D.C. loss model.

3.3.3 BALJE-BINSLEY LOSS MODEL

INTRODUCTION :-

To analyse the distribution of losses in the annulus of a turbine, it is essential to seperate the losses into its principal constituents, namely. The profile losses and the secondary losses. A survey and comparision of methods for predicting the profile loss of turbine blade had been carried out by J.D. DENTON (30). He discussed the factors affecting the profile losses of turbine blades and various methods of

predicting the loss from simple blade parameters. The methods
are compared with cascade results and it is found that none
of them predicts the loss very accurately. Balje and Binsley
method was considered the best having a standard deviation of
0.36 in value of (Predicted loss-experimental loss).

Balje-Binsley derived a generalized loss correlation
& critically compared with recently published data. Effect
included were reynolds number, blade angle, blade height,

number of blades, blade trailing edge thickness, tip
clearance and degree of reaction. These generalized loss
relationships are for use in optimization of turbines over a
wide range of possible operating conditions. The correlation
express losses as a function of key geometrical parameters.
When the expressions for all significant losses are combined,
it becomes possible to find the particular geometry which
maximizes efficiency for a particular set of operating conditions.

3.3.4 LOSS RELATIONS :-

CASCADE LOSSES :-

A typical cascade loss distribution is presented in
fig. No. (5), which shows that two frictional loss sources
have to be distignished in typical cascade :

(a) The profile losses, this loss in a turbine blading is due
to the boundary layer growth on the blade surface and due
to dissipation in the blade wake. In a real machine this

loss can not be isolated from other sources of loss so prediction of profile loss are always based on and compared with the tests made in a cascade tunnel. In such tests the profile loss is taken to be the loss in the region unaffected by the secondary flow near the end walls.

(b) The end wall losses are caused by the difference of pressure between suction and pressure side of the profile near the end walls. In addition clearance losses, due to the finite gap between rotor blades and stationary casing.

3.3.5 <u>PROFILE LOSSES</u> :-

The approach for the calculation of profile losses is to calculate the pressure and velocity distribution around the profile, then to calculate the boundary layer displacement and momentum thicknesses which are the measure of profile losses. To apply this procedure, definite profile shapes have to be assumed first. An early approach was presented by Zweifel (27), who argued that the actual velocity distribution around the cascade could be approximated by a rectangular distribution. Zweifels (27) Analysis was not able to produce an acceptable interrelation between the referred boundary-layer momentum thickness and cascade geometry. Losses predicted by this method were very high. An alternative approach used in this regard is to assume a different form of surface velocity distribution, then calculate the boundary layer momentum thickness based on that distribution. The surface velocity

has been assumed by Balje & Binsley (27) to vary linearly,
with camber line length from the leading edge to the trailing
edge. The Truckenbrodt's expression for the momentum thick-
ness can be given as

$$\Theta \left(\frac{C_2 \Theta_2}{\nu_2} \right)^{\cdot} = C_2^{-3-\frac{2}{n}} A \int_{x=0}^{x=1} C^{3+\frac{2}{n}} dx \qquad \text{\_\_\_\_\_(4.0)}$$

n is a constant (n = 3 to 6), which depends essentially
on Reynolds number. To apply this equation we should know the
variation of surface velocity C with distance x. By making
several assumptions this may be visualized as on approximately
trapezoidal free stream surface velocity distribution. Thus,
for a constant blade height along the flow path surface
velocity is given by

$$C = C_2 \left[\frac{\text{Sin } \beta_2}{\text{Sin } \beta_1} + \frac{x}{\ell} \left(1 - \frac{\text{Sin } \beta_2}{\text{Sin } \beta_1} \right) \right] \qquad \text{\_\_\_\_(4.1)}$$

Substituting equation (4.1) into (4.0) rearranging and
integrating

$$\frac{\Theta}{l} = \frac{\left(\dfrac{A}{4+\frac{2}{n}} \right)^{\frac{n}{n+1}}}{\left(\dfrac{C_2 l}{\nu_2} \right)^{\frac{1}{n+1}}} \left[\frac{1 - \left(\dfrac{\text{Sin } \beta_2}{\text{Sin } \beta_1} \right)^{4+\frac{2}{n}}}{1 - \dfrac{\sin \beta_2}{\text{Sin } \beta_1}} \right]^{\frac{n}{n+1}} \qquad \text{\_\_\_\_(4.2)}$$

Assuming n=4 and including the terms A & $C_2 l/\vartheta_2$ in a constant 'K' the final relation for momentum thickness can be written as

$$\theta/l = K \left[\frac{-\left(\frac{\sin \beta_2}{\sin \beta_1}\right) 4.5}{\left(1 - \frac{\sin \beta_2}{\sin \beta_1^2}\right)} \right]^{0.8} \qquad \underline{\qquad} (4.3)$$

or $\quad \theta/l = K \left[\frac{1-(\sin R) 4.5}{1-(\sin R)} \right]^{.8} \qquad \underline{\qquad} (4.4)$

where the value of constant K = 0.0021

Now $\quad \theta^* = \theta/l \times 1/b_c \times \dfrac{b_s}{b_s \times \sin \beta_2} \qquad \underline{\qquad} (4.5)$

and $\quad \delta^* = H \, \theta^*$

where H is the shape factor which can be calculated as follows :

$$H = \frac{\dfrac{1}{n+1} + \dfrac{3A_{fs}}{3n+1} + \dfrac{5A_{fs}^2}{5n+1} + - - - -}{\dfrac{1}{(n+1)(2n+1)} + \dfrac{\bar{A}_{fs}}{(3n+1)(4n+1)} + \dfrac{A_{fs}^2}{(5n+1)(6n+1)} + - - -}$$

If $\left(\dfrac{V}{V_{cr}}\right)$ then $\quad H = \dfrac{\dfrac{1}{n+1}}{\dfrac{1}{(n+1)(2n+1)}}$

$\qquad \underline{\qquad} (4.6)$

or $\quad H = (2n+1)$

Now the profile loss coefficient can be given as follows :

$$\zeta_p = \frac{Cos^2 \beta_2 (1- \delta^* - \theta^* - \frac{t_e}{b_s})^2 + Sin^2 \beta_2 \left(1 - \delta^* - \frac{t_e}{b_s}\right)^2}{1.0 - \frac{(1 - \delta^* - \frac{t_e}{b_s})^2}{1 + 2Sin^2 \beta_2 (1 - \delta^* - \frac{t_e}{b_s})^2 - (1 - \delta^* - \theta^* - \frac{t_e}{b_s})}} \quad \underline{\hspace{1cm}} (4.7)$$

This expression is for the incompressible flow . ·

3.3.6 <u>END WALL LOSSES</u> :-

The endwall losses may be attributed to two different flow mechanisms, one is the boundary layer build up along the wall at both tip and hub sections as flow passes from inlet to the exit of the cascade. The other is the secondary or cross flow effect which tends to move the fluid across the channel from pressure **surface** to the suction surface of the adjacent blade. The following loss correlation has been given for minimum loss coefficient.

$$h/c \;\; \zeta_e = K_e \left\{ \left[.0388 \left(\frac{Sin \beta_2}{Sin \beta_1} + 0.08 \right) (1 + \frac{\beta_1 - \beta_2}{100}) \right] \right.$$

$$\left. + .000337 \left[10 \frac{Sin \beta_2}{Sin \beta_1} + 0.08 \right]^{1.5} + \frac{\lambda_1 - \lambda_2}{160} \right. \quad \underline{\hspace{1cm}} (4.8)$$

With K_e = 0.3 for nozzle

and

K_{cr} = 0.3 + tanh (2.857 M ζ_{em}) for the rotor blade.

3.3.7 **TIP CLEARANCE LOSS :-**

This loss is due to the pressure difference between the pressure and suction side of the profile and the leakage flow over the tip of the blade. The emperical relation for this is given as

$$\zeta_{CL} = \ell_s \frac{C_R}{D} \; \frac{D}{h} \; \sin\beta_\infty \; \delta_u R \qquad \text{------- (4.9)}$$

where ℓ_s = 0.0696 tanh $(13 \; S/_{CR})$

4.0.0 **BALJE-BINSLEY WITH DUNHAM-CAME LOSS MODEL (B.B.D.C.) :-**

Balje-Binsley loss model underpredicts the secondary losses, because the selection of this new set of loss-relationship is to describe the axial flow turbines with optimum solidity. This loss relationship are primarily meant for optimum design of turbines over a wide range of the possible operating conditions. So in practice, however the secondary losses are likely to be higher than predicted by Balje Binsley correlation. To overcome this limitation, present work has a combination of loss-models of Balje-Binsley (for profile losses) and Dunham-Came, (for secondary losses). This correlation has been found/to give good agreement with the experimental results of the highly loaded multistage turbines.

CHAPTER - 4

"COMPUTER PROGRAM"

4.1 INTRODUCTION :-

The basic equations which governs the design point
performance of axial turbine have been discussed in the previous
chapters. These equations must be solved by numerical methods
which can be lengthy and time consuming. Therefore, it is
of considerable importance that they be solved using a digital
computer.

A program for gas turbine analysis was developed by
Govindan (39). However the computer deck of this program was
not available as the original program had been modified for
the analysis of steam turbines. A considerable effort was
spent to modify this steam turbine program for the case of
gas turbine analysis. This program is written in Fortran IV
language and is capable of analysing both single and multispool
units. A maximum of three spool is allowed, and each spool
may have up to 8 stages. The absolute and relative flow fields
are computed at the first stator inlet, at each inter blade
row plane, and at the final rotor exit. The effect of the
radial variation of the following quantity are taken into
account : Inlet conditions, streamline angle of inclination
and curvature, loss coefficient or efficiency, whirl velocity
and axial velocity. The effect of the coolent flow and

interfilament mixing, and a station to station variation of the specific heat has been included. As additional feature, the program allows for the internal calculation of losses based on the correlations. Any of the correlation can be used by changing the value of an index (IPLC) in the input data.

4.2 DESCRIPTION OF INPUT DATA :-

The general specification of turbine consists of

1. Number of spool

2. Gas constant of working fluid

3. Mass flow at the turbine inlet

4. Flow conditions at inlet of turbine (Total temperature, total pressure, and flow angles as a function of radius).

The spool specification consist of

1. Rotative speed

2. Rotor exit relative angles

Finally, The spool analysis variable consist of

1. Number of stages

2. Rotor relative exit angles

3. Specific heats and spool inlet and each blade row exit station.

4. Annulus geometry and axial position of each station.

5. Mass flow and total temperature of coolent added if the turbine is cooled.

6. Streamline value of mixing coefficient for each blade row if interfilament mixing is specified.

7. Whirl velocity or flow angle as a function of radius at each stator exit.

8. Stream line value of the power output distribution or the rotor relative exit angles.

9. Stage efficiency, rotor efficiency, total pressure loss coefficient or kinetic energy loss coefficient, when the losses are not calculated from the loss correlation available in the program.

4.3 DESCRIPTION OF NORMAL OUTPUT :-

The output of the program consists entirely of printed data. This can be listed as follows :

1. All input data

2. Tabulated streamline values of flow parameters

3. Tabulated streamline values of mixed and/or cooled flow parameters for a blade row.

4. Tabulated streamline values of the performance parameters of the stator and rotor blade rows.

5. Mass averaged performance parameter for a stage.

6. Tabulated mass averaged performance parameters for each stage of spool.

7. Mass averaged performance parameter for a spool.

8. Mass averaged performance parameter for the turbine.

9. In addition streamline values of the flow parameters

through each iteration of the computation can also be printed if desired.

The most serious problem of this program is the mass flow convergence, at stations where the choking flow accured and resulted in oscillation of the solution and consequent abandoning of the calculation. The reason for these oscillation was too large a change in the meriodional velocity from one iteration to the next of the inner loop. This resulted in the mass flow oscillating about the choking mass flow without convergence. The solution of this problem was to use the damping techniques on the meriodional velocity

$$V_m^{(2)} = V_m^{(1)} + (1- \lambda) V_{m1}^{(2)} \underline{\qquad} (4.1)$$

where $V_{m\,1}^{(2)}$ is the value of meriodional velocity calculated for the new iteration, $V_m^{(1)}$ value for the previous iteration. $V_m^{(2)}$ value used in new iteration which is the damped value. The value of λ between 0.7 to 0.8 to effectively damp the oscillation.

In this program use of the rotor relative exit angles has been made instead of the work specification.

4.4 OVER-ALL PROGRAM LOGIC :-

The computer program is composed of a main routine and twenty three subroutines. A list of these subroutines along with their function is as follow :

1. INPUT :- To print all the input data

2. STRAC :- To calculate the slope & curvature of the hub & casing stream lines.

3. SPECHT :- To determine the specific heats at constant pressure, specific heat ratio & related parameter at each station.

4. POWER :- To determine the drop in absolute total temperature across each stream lines of a rotor when work done by the turbine is specified.

5. POWER 1 :- To determine the drop in absolute total temperature across each stream line of a rotor when rotor exit relative angles are specified.

6. STRIP :- To obtain the initial estimate of the radial position of each stream line.

7. STRVAL :- To obtain the stream line value of the items required for the solution of radial equilibrium equation.

8. VMNTL : To obtain the initial estimate of the meriodional velocity at the mean stream line.

9. RADEQL :- To control the logic of the calculation of the meriodional velocity distribution.

10. RUNKUT :- Contains the algorithms for the Runga-Kutta Gill Method for solving the Ist order ordinary differential equation.

11. DERIV :- To obtain a value of the derivative of the square of the meriodional velocity with respect to radial position for a specified velocity & radial position.

12. VMSUB :- To obtain the new estimate of meriodional velocity at mean stream line.

13. REMAIN :- To obtain the stream line value for the quantity tabulated in the output which have not already been obtained.

14. SETUP :- To obtain the stream line value of quantity for calculation at next station. If also calculates the mass averaged value which are to be printed in the output.

15. OUTPUT :- To print the result of the calculations.

16. PLC :- To evaluate the total pressure loss coefficients for each stream line using the loss model.

17. PLC_1 :- To evaluate the total pressure loss coefficient for each stream line using the loss model developed for Balje-Binsley loss model.

18. LCNV :- To estimate the total pressure loss coefficient from the kinetic energy loss coefficient when they are specified.

19. SPLINE :- To evaluate stream line slope & curvature by filting spline curve through the estimated stream line radial position.

20. I1AP1 :- To perform parabolic Interpolation of a tabulated function of one variable if parabolic interpolation is not possible, linear Interpolation or Extrapolation of a single value is performed.

21. SLOPE :- To obtain the derivative of a tabulated function with respect to an independent variable at each tabular entry.

22. SIMEQ :- Solution of a set of simaltaneous linear

algebric equation by Gauss method, with pivoting.

23. PLC_2 :- Modified internal loss correlation of pressure

loss coefficient replacing the subroutine PLC_2 and to

evaluate the total pressure loss coefficient for each stream

line by using modified form of the AMDC loss model.

An overall flow diagram for the program is given

in figure (4). The overall control of the calculation

procedure is maintained by the main routine.

The results obtained from using the above computer

program have been plotted by using the graphic terminal. A

seperate program is used to plot these curves. By using

computer program each data can be taken to a very good

accuracy. Curves plotted on a graphic terminal are more

accurate than plotting these curves manually.

CHAPTER - 5

RESULTS AND DISCUSSION

The computer program discussed in the previous chapter is used to evaluate the performance of a signle stage, three stage, and four stage turbines having very high stage loading factor. In this chapter the computed results with different loss models have been compared with the available experimental data for these turbines.

5.1   TEST CASE 1 :-

For the first test case a single stage turbine was used (Ref. 31). The velocity triangles and the turbine flow path for this turbine are presented in the figure No. 6. The program was run with the specified rotor relative exit angles and design mass flow rate for each loss model, computed results are plotted, for both design and off-design calculations.

Fig. (7) shows the stage exit total pressure distribution with hub to tip radius ratio. It is concluded from the graphs that the Carter's (21) loss model and BBDC loss model are close to the experimental curve as compared to the Balje-Binsley and Kacker Okapuu loss models. Fig. (8) presents the radial distribution of outlet flow angles. This again indicates that Carter's (21) loss model is the closest one to the experimental curve than the other loss model. These curve shows that the effect of the loss distribution is less important in case of

the large hub-to-tip radius ratio turbines which have small
blade heights. Fig. 9 shows the radial distribution of the
total to total efficiency. In this figure the efficiencies
obtained using the four loss models are compared. Carter's (21)
loss model shows the maximum efficiency at the tip while the
other loss-models give the minimum efficiency at the hub and
maximum efficiency around the mean line as would be expected
in an axial turbine. Maximum efficiency at the tip is unlikely
to occur in a turbine. The efficiency plot shows the difference
in the loss-distributions of each loss model. Fig. 10 shows
the comparision of the off design calculations in which the
total to total pressure ratio is plotted against the equivalent
weight flow. Balje-Binsely loss model, Kacker-Okapuu loss
model and BBDC loss model shows a close agreement with the
experimental results. The design mass flow is 2.507 kg/sec
with total to total pressure ratio of 1.90.

The results for the experimental and for all the loss
model have been summarised in the following table :-

TABLE - 1

	Experimental	Carter's (21) loss model	Balje-Binsley loss model	Kacker-Okapuu loss model	BBDC loss model
(1) Spool Work					
(a) With Design Pressure ratio	43.23	41.534	42.774	42.550	41.871
(b) With Design Mass Flow		48.164	41.058	42.550	44.946
(2) Turbine total Efficiency					
(a) With Design Pressure Ratio	0.92	0.922	0.958	0.9501	0.934
(b) With Design Mass Flow		0.923	0.959	0.9501	0.933
(3) Total to Total Pressure Ratio					
(a) With Design Pressure Ratio		1.807	1.796	1.80	1.80
(b) With Design Mass Flow	1.909	2.00	1.75	1.80	1.89
(4) Hub Static Pressure					
(a) With Design Pressure Ratio		0.512	0.515	0.50	0.51
(b) With Design Mass Flow	0.455	0.455	0.529	0.50	0.48
(5) Tip Static Pressure					
(a) With Design Pressure Ratio		0.497	0.498	0.49	0.49
(b) With Design Mass Flow	0.445	0.435	0.514	0.49	0.46

From the Table 1 it is clear that BBDC and Kacker-Okapuu loss model gives result close to the experimental values. Carter's loss model predicts a higher total to total pressure ratio, and a higher work extraction. Balje-Binsley loss model also gives comparable results for this case, Denton (30) suggested that a comparision can be made by keeping the design pressure ratio fixed. Which is an important design parameter for turbine. On this basis also all the loss models give a good comparision.

5.2 TEST CASE 2 :-

In the second test case a three stage(highly loaded) turbine was used. The design details for this turbine have been collected from Ref. (34). Some of the design details are presented in Fig. 11 and the turbine flow path has been shown in fig. 12.

In Figures 13, 14 and 15, the hub and tip pressure distributions for different axial stations have been plotted for Carter's (21), Kacker-Okapuu and BBDC loss models and each one is compared with the experimental results separately, Kacker-Okapuu and BBDC loss model have very close agreement with the experimental results.

Fig. 16 presents the total to total efficiency distribution with percentage blade height. This figure compares the AMDC loss-model used by Govindan(39) with the

loss models of the present work, Kacker-Okapuu and BBDC
loss model show better agreement with the experimental results.
All loss models give the maximum efficiency around the mean
line as would be expected in an axial turbine. This figure
gives an interesting information regarding the AMDC loss
model used by Govindan (39). While the original AMDC loss
model underpredicts the overall efficiency, the modified AMDC
loss model of Kacker and Okapuu overpredicts by 2%. Fig. 17
shows the axial velocity distribution at the entry of the
last stage of the turbine. This distribution is parabolic.

Fig. 18 presents a plot of equivalent specific work
against the total to total pressure ratio. Kacker-Okapuu and
BBDC loss models are very close to the experimental results.
Balje-Binsley loss model under predicts the losses, while the
modified Balje-Binsley loss model (BBDC) gives a good agreement.
The carter's (21) loss model failed to give a conversed
solution for highly loaded three stage turbine. The solution
is sensitive to the radial distribution of losses. The results
for this loss model have been taken at reduced mass flow rate.
This predicts the lowest value of the specific work for a
given total to total pressure ratio. In figure 19 the equivalent
weight flow vs. total to total pressure ratio has been plotted.
The trend of curve for Carters loss model(21) indicate that this
loss model is not suited for multistage turbines although it
may give reasonable results for high hub to tip radius ratio
single stage turbines. Again the Kacker-Okapuu and BBDC loss

model have the closest agreements with the experimental results. For the same design mass flow the Kacker and Okapuu loss model gives slightly higher total to total pressure ratio. Balje-Binsley loss model has a lower value of total/total pressure ratio for the design mass flow. Table 2 compares the predicted overall performance parameters with experimental results.

P.T.O.

TABLE — 2

	Experimental	Carter's (21) loss model	Balje Binsley loss model	Kacker Okapuu loss model	BBDC loss model
(1) Spool Work					
(a) With Design Pressure Ratio		94.239	108.342	104.353	103.833
(b) With Design Mass Flow	103.589	86.898	104.353	112.669	
(2) Turbine Total Efficiency					
(a) With Design Pressure Ratio		0.822	0.921	0.91	0.90
(b) With Design Mass Flow	0.889	0.943	0.91	0.905	
(3) Total To Total Pressure Ratio					
(a) With Design Pressure Ratio		3.366	3.357	3.363	3.355
(b) With Design Mass Flow	3.48	2.56	3.368	3.83	
(4) Total To Static Pressure Ratio					
(a) With Design Pressure Ratio		3.723	3.75	3.75	3.73
(b) With Design Mass Flow	3.843	3.792	2.72	4.45	

In the table 2, Balje-Binsley loss model indicates that it underestimates the loss because it is giving the very high efficiency lowest total to total pressure ratio and lowest work extraction. Kacker and Okapuu shows a very close result to the experimental result. A comparision on the basis of the design pressure ratio shows that BBDC loss model has a good agreement with the experimental results. Design mass flow has been reduced by 0.7% in this case to get the design pressure ratio. For the Carter's loss model design mass flow has been reduced by 6% to get the design pressure ratio. This model predicts very low efficiency.

5.3 Test Case 3 :-

In this test case, A four stage turbine with very high stage loading was used. Design details for this turbine have been taken from Ref. (33).Some of the design details are given in the fig. (20) and fig. (21).

The fig. (22) describes the radial variation of the stage exit total pressure for the design mass flow rate. This shows that for the same radius ratio, each loss model has a quite different value of pressure ratio. Further in Fig.(23) same graphs is plotted with design pressure ratio. Here for the same value of the radius ratio every loss model has a very close value of pressure ratio to each other. The BBDC loss model and Kacker-Okapuu loss models have almost the same value of the pressure ratio for the same radius ratio. Fig.(24)

gives the radial variation of the outlet flow angles. In most cases, there is a good agreement with the experimental results.

Fig. 25 compares, the equivalent specific work Vs total to total pressure ratio. For the design pressure ratio, BBDC loss model and Kacker-Okapuu loss model gives very close values of the equivalent specific work, which is almost matching with the experimental results. Balje-Binsley loss model gives a higher value of the specific work than the experimental value. Carter at. al. loss model is not able to give the solution for design mass flow rate due to convergence problems.

Fig. 26 explains the comparision of various loss models with experimental results for off design calculations. This figure shows the variation of equivalent weight flow with total to total pressure ratio. In general there is a good agreement with experimental results. For the design mass flow rate BBDC loss model has the maximum value of total to total pressure ratio.

Fig. 27 gives the variation of the efficiency with total to total pressure ratio. This shows that for the design pressure ratio, present loss models have higher values of efficiency than the experimental values. Balje-Binsley loss correlation shows the maximum value of efficiency, this

clearly indicates that this loss model underpredicts the losses.

Fig. 28, Fig. 29 and Fig. 30 present stage to stage hub and tip static pressure distributions in the turbine. In most cases there is a good prediction of the wall static pressure distribution. Table 3 compares the predicted overall performance parameter with experimental results.

Table 3 shows a comparision on the basis of the design pressure ratio for this test case give that BBDC and Kaker-Okapuu are the best loss models. For the BBDC loss model there is a 1% reduction in the design mass flow. While in case of the Balje-Binsley there is 4.5% increase in the design mass flow in order to get the design pressure ratio. For Carter's loss model there is 8% reduction in mass flow.

TABLE — 3

	Experimental	Carter's(21) Loss model	Balje Binsley Loss model	Kacker Okapuu BBDC Loss model
(1) Spool Work				
(a) With Design Pressure Ratio	80.301	98.537	92.165	90.685
(b) With Design Mass Flow	88.255	78.697	92.165	101.568
(2) Turbine Total Efficiency				
(a) With Design Pressure Ratio	0.745	0.917	0.856	0.843
(b) With Design Mass Flow	0.853	0.933	0.856	0.830
(3) Total To Total Pressure Ratio				
(a) With Design Pressure Ratio	2.783	2.777	2.78	2.779
(b) With Design Mass Flow	2.79	2.16	2.78	3.28
(4) Total To Static Pressure Ratio				
(a) With Design Pressure Ratio	3.16	3.32	3.258	3.24
(b) With Design Mass Flow	2.955	2.34	3.258	4.39

CONCLUSIONS

1) Four different loss models have been used in a streamline curvature computing scheme to study their suitability in predicting the performance of axial turbines. The computed results have been compared with experimental results for three test cases which include three and four stage turbines. The results have been obtained both at design mass flow rate and design pressure ratio. Off-design performance is also studied by varying the mass flow rate at the design r.p.m.

2) The modified AMDC loss correlation by Kacker and Okapuu has been found to give results in good agreement with experimental values. The predicted efficiencies are slightly (2 to 3%) higher than the experimental values. The original AMDC loss model used by Govindan (39) under predicted the efficiencies.

3) Balje-Binsley correlation tends to predict low loss levels and therefore higher efficiencies. This is mainly due to the low values of secondary losses predicted by this model. However when Balje-Binsley profile loss correlation was combined with Dunham and Came secondary loss correlation (BBDC los Model), the predicted results were closest to experimental results.

4) Carter's loss model is mainly suited for single stage turbines with high hub to tip radius ratio.

Appendix A

An expression for the term $D\,V_m/Dm$ in the radial equilibrium equation

The continuity equation can be written as :

$$\frac{W}{\rho}\ \frac{D}{Ds} + \nabla \cdot \vec{W} = 0 \tag{A1}$$

In cylindrical co-ordinates,

$$\nabla \cdot \vec{W} = \frac{1}{r} \cdot \frac{\partial(r\,W_r)}{\partial r} + \frac{\partial W_u}{r\,\partial\theta} + \frac{\partial W_x}{\partial x} \tag{A2}$$

Also, the derivative of a quantity in the direction of flow

(the s-direction) at any instant in time may be expressed by :

$$\frac{\partial(\ )}{\partial s} = \frac{W_r}{W} \cdot \frac{\partial(\ )}{\partial r} + \frac{W_u}{W}\ \frac{\partial(\ )}{r\,\partial\theta} + \frac{W_x}{W} \cdot \frac{\partial(\ )}{\partial x} \tag{A3}$$

or re-arranging,

$$\frac{\partial(\ )}{\partial x} = \frac{W}{W_x} \cdot \frac{\partial(\ )}{\partial s} - \frac{W_r}{W_x} \cdot \frac{\partial(\ )}{\partial r} - \frac{W_u}{W_x} \cdot \frac{\partial(\ )}{r\,\partial\theta} \tag{A4}$$

Use equation (A4) in (A2) to eliminate the x derivative.

We get

$$\nabla \cdot \vec{W} = W_x \left\{ \frac{1}{r} \cdot \frac{\partial}{\partial r} \left(\frac{r W_r}{W_x} \right) + \frac{\partial}{r\,\partial\theta} \left(\frac{W_u}{W_x} \right) + \frac{W}{W_x} \cdot \frac{\partial W_x}{\partial s} \right.$$

$$\tag{A5}$$

Since,

$$\frac{W_r}{W_x} = \tan\phi \quad \text{and} \quad \frac{W_u}{W_x} = \tan\beta$$

equation (A5) can be rewritten as

$$\nabla \cdot \vec{W} = W_x \left[\frac{1}{r} \cdot \frac{\partial(r \tan \phi)}{\partial r} + \frac{\partial \tan \beta}{r \partial \theta} \right] + \frac{W}{W_x} \cdot \frac{\partial W_x}{\partial s} \quad \text{(A6)}$$

It is known that

$$\frac{D(\ )}{Dt} = \frac{\partial(\ )}{\partial t} + W \frac{\partial(\ )}{\partial s} \quad \text{(A7)}$$

Along with the kinematic relation $\frac{D(\ )}{Dt} = \frac{D(\ )}{Ds}$, equation (A7) can be written

$$\frac{\partial(\ )}{\partial s} = \frac{D(\ )}{Ds} - \frac{1}{W} \cdot \frac{\partial(\ )}{\partial t} \quad \text{(A8)}$$

Equation (A8) can be used for the last term of equation (A6). Also since

$$W_x = W_m \cos \phi \quad \text{(A9)}$$

we get,

$$\frac{\partial W_x}{\partial s} = \frac{D}{Ds} (W_m \cos \phi) - \frac{1}{W} \cdot \frac{\partial W_x}{\partial t} \quad \text{(A 10)}$$

We also know that

$$W \frac{D(\ )}{Ds} = W_m \frac{D(\ )}{Dm} \quad \text{(A11)}$$

Thus,

$$\frac{\partial W_x}{\partial s} = \frac{W_m^2}{W} \cdot \frac{D \cos \phi}{Dm} + \cos \phi \frac{W_m}{W} \cdot \frac{DW_m}{Dm} - \frac{1}{W} \cdot \frac{\partial W_x}{\partial t} \quad \text{(A 12)}$$

Substitute equation (A12) in (A6), we get

$$\nabla \cdot \vec{W} = W_x \left[\frac{1}{r} \cdot \frac{\partial(r \tan \phi)}{\partial r} + \frac{\partial \tan \beta}{r \partial \theta} \right] + W_r \frac{\sec \phi}{r_m} + \frac{DW_m}{Dm}$$
$$- \frac{1}{W_x} \cdot \frac{\partial W_x}{\partial t} \quad \text{(A13)}$$

For an axisymmetric, steady flow

$$\nabla \cdot \vec{W} = W_x \; \frac{1}{r} \; \frac{\partial(r \tan \phi)}{r} + W_r \; \frac{\sec \phi}{r_m} + \frac{DW_m}{Dm} \qquad (A14)$$

We next apply the momentum equation in the flow direction

$$-\frac{W}{\rho} \cdot \frac{\partial p}{\partial s} = \frac{D}{Dt}\left(\frac{W^2}{2}\right) - \omega^2 \, rW \qquad (A15)$$

Using equations (A8) and (A11), (A15) can be written as

$$-\frac{W}{\rho} \cdot \frac{Dp}{Ds} + \frac{1}{\rho} \cdot \frac{\partial p}{\partial t} = W_m^2 \; \frac{DW_m}{Dm} + W_u W \frac{DW_u}{Dx} - \omega^2 \, rW \qquad (A16)$$

This can be rewritten as

$$-\frac{W}{\rho} \cdot \frac{Dp}{Ds} = W_m^2 \; \frac{DW_m}{Dm} - W_r \; \frac{V_u^2}{r} - \frac{W_u}{\rho} \cdot \frac{\partial p}{r\partial\theta} - \frac{1}{\rho} \cdot \frac{\partial p}{\partial t} \qquad (A17)$$

For an axisymmetric, steady flow

$$-\frac{W}{\rho} \cdot \frac{Dp}{Ds} = W_m^2 \; \frac{DW_m}{Dm} - W_r \; \frac{V_u^2}{r} \qquad (A18)$$

Also,

$$\frac{Dp/Ds}{D\rho/Ds} = a^2 \qquad (A19)$$

This relation along with equation (A1), (A14), and (A18) can be used to obtain an expression for DW_m/Dm that does not contain $\nabla \cdot \vec{W}$, Dp/Ds or $D\rho$/Ds. We get

$$\frac{1}{a^2}\left[W_r \; \frac{V_u^2}{r} - W_m^2 \; \frac{DW_m}{Dm}\right] + \frac{W_x}{r} \cdot \frac{\partial(r \tan \phi)}{\partial r} + W_r \; \frac{\sec \phi}{r_m} + \frac{DW_m}{Dm} = 0$$

$$(A20)$$

Using the definition of Mach number, $M_m = W_m/a$ and $M_\ominus = V_u/a$

in equation (A20) and rearranging, we get

$$(1- M_m^2) \ \frac{DW_m}{Dm} = W_m \left[\frac{M_\ominus^2}{r} \sin\phi + \frac{\tan\phi}{r_m} + \frac{\sin\phi}{r} + \frac{1}{\cos\phi} \cdot \frac{\partial\phi}{\partial r} \right]$$

$$(A.21)$$

Since $W_m = V_m$, equation (A21) can be rewritten as

$$\sin\phi \ \frac{DV_m}{Dm} = \frac{V_m \left[(1+ M_\ominus^2 + \frac{r}{r_m \cos\phi}) \frac{\sin^2\phi}{r} + \tan\phi \frac{\partial\phi}{\partial r} \right]}{(1 - M_m^2)}$$

$$(A.22)$$

Appendix B

Evaluation of the total temperature drop
across a stage

When the total power output of a stage is specified,
the total temperature distribution at a stage exit will have
to satisfy both the specified power output and its distribution
across the annulus. Since initially the distribution of mass
flow throughout the annulus is unknown until the distribution
of meridional velocity has been established, the power
distribution is specified by nondimensional power functions
versus the nondimensional mass flow function, $w(r)$, defined
below

$$w(r) = \frac{2\pi \int_{r_h}^{r} \rho \, V_x \, r \, dr}{w_T} \qquad (A23)$$

If the total power output specified is HP_T (horsepower)
the total temperature drop ΔT_o through the rotor must satisfy
the equation,

$$HP_T = 5.6925 \; c_p \int_{o}^{w_T} \Delta T_o \, dw \qquad (A24)$$

Normalizing equation (A24) with respect to the total power
and the total mass flow, leads to a definition of the power
function $P(w(r))$ expressed as

$$P(w(r)) = 5.6925 \; w_T \, c_p / HP_T \int_{o}^{w(r)} \Delta T_o \, d \, w(r) \qquad (A25)$$

Differentiating equation (A25) with respect to the non-dimensional mass flow function yields an expression for the total temperature drop, for the jth streamline.

$$(\Delta T_o)_j = \frac{HP_T}{5.6925 \ W_T \ c_p} \left[\frac{dp(w(r))}{dw(r)} \right]$$ (A26)

The power function versus the mass flow function will be a basic specification for power distribution from which the total temperature drops are obtained.

When the rotor relative exit angles are specified, the total temperature drops are obtained from the Euler work equation

$$(\Delta T_o)_j = \left[\frac{V_{u1} \ u_1 - V_{u2} \ u_2}{c_p} \right]_j$$ (A27)

Appendix C

Coefficients of the differential equations

To simplify the logic of the computer program, a standard procedure has been adopted for the solution of the flow field at each inter blade row station. The different types of stations and the various optional specifications are taken into account by modifications to the twelve coefficient appearing in the three differential equations (Equations 2.30 2.31, and 2.32). This appendix presents these coefficients.

First station inlet

$$C_{11} = 1.0$$

$$C_{12} = (\frac{\gamma-1}{\gamma}) \left[V_{uo}^2 + V_{mo}^2 - 2c_p T_{oo} \right]$$

$$C_{13} = 2V_{uo}$$

$$C_{14} = \frac{2V_{mo}^2 \cos\phi_o}{V_m} - \frac{2V_{uo}^2}{r} + (V_{uo}^2 + V_{mo}^2) \frac{1}{T_{oo}} \frac{dT_{oo}}{dr} + V_{mo} \sin\phi_o \frac{DV_{mo}}{Dm}$$

The total pressure would be a specified function of radius. Hence, the coefficients of equation (2.31) are

$$C_{21} = 0$$

$$C_{22} = 1.0$$

$$C_{23} = 0$$

$$C_{24} = \frac{1}{p_{oo}} \cdot \frac{dp_{oo}}{dr}$$

$$C_{31} = - \frac{\tan \beta_o \cos \phi_o}{2V_{mo}}$$

$$C_{32} = 0$$

$$C_{33} = 1.0$$

$$C_{34} = V_{mo} \left[\frac{\cos \phi_o}{\cos^2 \beta_o} \frac{d\beta_o}{dr} - \tan \beta_o \sin \phi_o \frac{d\phi_o}{dr} \right]$$

Stator exit

$$C_{11} = 1.0$$

$$C_{12} = \left(\frac{\gamma-1}{\gamma} \right) \left[V_{u1}^2 + V_{m1}^2 - 2c_p T_{o1} \right]$$

$$C_{13} = 2V_{u1}$$

$$C_{14} = \frac{2V_{m1}^2 \cos \phi_1}{r_m} - \frac{2V_{u1}^2}{r} + (V_{u1}^2 + V_{m1}^2)\frac{1}{T_{01}} \frac{dT_{o1}}{dr}$$
$$+ V_{m1} \sin \phi_1 \frac{DV_{m1}}{Dm}$$

Assuming that the derivative $\frac{dY_N}{dr}$ can be expressed as

$$\frac{dY_N}{dr} = C_{Y1} \frac{dV_{m1}^2}{dr} + C_{Y3} \frac{dV_{u1}}{dr} + C_{Y4}$$

the coefficients of equation (2.31) become

$$C_{21} = \frac{(\frac{p_{o1}}{p_{oo}}) (\frac{T_1}{T_{o1}}) \frac{1}{\gamma-1}}{2R T_{o1}} Y_N + (\frac{p_{o1}}{p_{oo}}) (1- \frac{p_1}{p_{o1}}) C_{Y1}$$

$$C_{22} = 1.0$$

$$C_{23} = \frac{V_{u1} \left(\frac{p_{o1}}{p_{oo}}\right) \left(\frac{T_1}{T_{o1}}\right)^{\frac{1}{\gamma-1}}}{R\, T_{o1}} + \left(\frac{p_{o1}}{p_{oo}}\right)\left(1-\frac{p_1}{p_{o1}}\right) C_{Y3}$$

$$C_{24} = \frac{1}{p_{oo}} - \frac{dp_{oo}}{dr} + \frac{\left(\frac{p_{o1}}{p_{oo}}\right)\left(\frac{T_1}{T_{o1}}\right)^{\frac{1}{\gamma-1}}}{2R\, T_{o1}} \left(V_{u1}^2 + V_{m1}^2\right)\frac{Y_N}{T_{o1}}\frac{dT_{o1}}{dr}$$

$$- \left(\frac{p_{o1}}{p_{oo}}\right)\left(1-\frac{p_1}{p_{o1}}\right) C_{Y4}$$

$$C_{31} = -\frac{\tan \beta_1 \cos \phi_1}{2V_{m1}}$$

$$C_{32} = 0$$

$$C_{33} = 1.0$$

$$C_{34} = V_{m1} \left[\frac{\cos \phi_1}{\cos^2 \beta_1}\frac{d\beta_1}{dr} - \tan \beta_1 \sin \phi_1 \frac{d\phi_1}{dr}\right]$$

Stage exit

$$C_{11} = 1.0$$

$$C_{12} = \left(\frac{\gamma}{\gamma-1}\right) \left[V_{u2}^2 + V_{m2}^2 - 2c_p\, T_{o2}\right]$$

$$C_{13} = 2V_{u2}$$

$$C_{14} = \frac{2V_{m2}^2 \cos \phi_2}{r_m} - \frac{2V_{u2}^2}{r} + \left(V_{u2}^2 + V_{m2}^2\right)\frac{1}{T_{o2}} \cdot \frac{dT_{o2}}{dr}$$

$$+ V_{m2} \sin \phi_2 \frac{DV_{m2}}{Dm} \cdot$$

Again, assuming that the derivative $\frac{dY_R}{dr}$ can be expressed as

$$\frac{dY_R}{dr} = C_{Y1} \frac{dV_{m2}^2}{dr} + C_{Y3} \frac{dV_{u2}}{dr} + C_{Y4}$$

the coefficients of equation (2.31) are

$$C_{21} = \frac{(\frac{p'_{o2}}{p'_{o2s}}) Y_R}{2R\,T_2} + (\frac{p'_{o2}}{p'_{o2s}})(1 - \frac{p_2}{p'_{o2}}) C_{Y1}$$

$$C_{22} = 1.0$$

$$C_{23} = \frac{V_{u2}(\frac{p'_{o2}}{p'_{o2s}})Y_R}{R\,T_2} - \frac{u_2\left[1 - (\frac{p'_{o2}}{p'_{o2s}}) Y_R\right]}{R\,T'_{o2}}$$

$$+ (\frac{p'_{o2}}{p'_{o2s}})(1 - \frac{p_2}{p'_{o2}}) C_{Y3}$$

$$C_{24} = \frac{1}{p'_{o1}} \frac{dp'_{o1}}{dr} + \frac{1}{2R\,T'_{o2}}\left[2u_2\omega - wu_1\omega - \right.$$

$$\left. -(u_2^2 - u_1^2)\frac{1}{T'_{o1}} \frac{dT'_{o1}}{dr}\right]$$

$$- \frac{(1 + \frac{p'_{o2}}{p'_{o2s}} Y_R)}{2R\,T'_{o2}}\left[2u_2\omega - 2V_{u2}\omega - \right.$$

$$\left. -(u_2^2 - 2u_2 V_{u2}) \frac{1}{T_{o2}} \frac{dT_{o2}}{dr}\right]$$

$$+ \frac{Y_R (\frac{p'_{o2}}{p'_{o2s}})}{2R\,T_2} (V_{m2}^2 + V_{u2}^2) \frac{1}{T_{o2}} \frac{dT_{o2}}{dr}$$

$$- (\frac{p'_{o2}}{p'_{o2s}})(1 - \frac{p_2}{p'_{o2}}) C_{Y4}.$$

When the work output of the turbine is specified, V_{u2} is in effect a known function of radius. Thus,

$$C_{31} = 0$$

$$C_{32} = 0$$

$$C_{33} = 1.0$$

$$C_{34} = \frac{dV_{u2}}{dr}$$

When the rotor relative exit angles are specified, the coefficients of equation (2.32) are similar to those at the stator exit.

$$C_{31} = - \frac{\tan \beta_2' \cos \phi_2}{2 \, V_{m2}}$$

$$C_{32} = 0$$

$$C_{33} = 1.0$$

$$C_{34} = V_{m2} \left[\frac{\cos \phi_2}{\cos^2 \beta_2'} \frac{d\beta_2'}{dr} - \tan \beta_2' \sin \phi_2 \frac{d\phi_2}{dr} \right]$$

Appendix D

The Runge-Kutta-Gill method for the solution of ordinary differential equations

The differential equation is of the form

$$dV_m^2/dr = f(r, V_m)$$

where $f(r, V_m)$ is obtained from the simultaneous solution of the radial equilibrium equation and two subsidiary differential equations.

Given the value of the meridional velocity at one streamline, $(V_{mi})_j$, the unknown value at the adjacent stream-line, $(V_{mi})_k$, is determined in four stages :

(1) $$(V_{mi})_{k1}^2 = (V_{mi})_j^2 + \tfrac{1}{2}(k_1 - 2q_o)$$

where $k_1 = hf\left\{ r_{ij}, \ (V_{mi})_j \right\}$

$$q_o = \begin{cases} 0 \text{ initially} \\ q_4 \text{ subsequently} \end{cases}$$

$$h = r_{ik} - r_{ij}$$

(2) $$(V_{mi})_{k2}^2 = (V_{mi})_{k1}^2 + (1 - \tfrac{1}{\sqrt{2}})(k_2 - q_1)$$

where $k_2 = hf\left\{ r_{ij} + h/2, \ (V_{mi})_{k1} \right\}$

$$q_1 = q_o + 3\left[\tfrac{1}{2}(k_1 - 2q_o) \right] - \tfrac{1}{2}k_1$$

(3) $\quad (V_{mi})^2_{k3} = (V_{mi})^2_{k2} + (1 + \frac{1}{\sqrt{2}}) \ (k_3 - q_2)$

where $\quad k_3 = hf \left\{ r_{ij} + h/2, \ (V_{mi})_{k2} \right\}$

$q_2 = q_1 + 3 \left[(1 - \frac{1}{\sqrt{2}}) (k_2 - q_1) \right] - (1 - \frac{1}{\sqrt{2}}) \ k_2$

(4) $\quad (V_{mi})^2_k = (V_{mi})^2_{k3} + \frac{1}{6} \ (k_4 - 2q_2)$

where $k_4 = hf \left\{ r_{ik}, \ (V_{mi})_{k3} \right\}$

$q_3 = q_2 + 3 \left[(1 + \frac{1}{\sqrt{2}}) (k_3 - q_2) \right] - (1 + \frac{1}{\sqrt{2}}) \ k_3$

$q_4 = q_3 + 3 \left[\frac{1}{6} (k_4 - 2q_3) \right] - \frac{1}{2} \ k_4 \ .$

<u>REFERENCES</u>

1. Merchant W. and Collar A.R., Flow of an Ideal fluid past a cascade of blades. Aero. Research Council R. and M. No. 1893 (1941).

2. Gostelow, J.P., Potential flow through cascade, Extension to an exact theory, Aero. Research Council 808, (1964).

3. Martensen E. , Calculation of pressure distribution over profiles in cascade in 2-D potential flow by means of Fredholm integral equation. Arch. for Rat. Mech. and Anal. Vol. 3, No. 3 (1959).

4. Wilkinson, D.H. A Numerical Solution of the analysis and design problem for the flow past one or more Aerofoils in cascade, Aero. Research Council, R. & M. 3545 (1968)

5. Von, Karman T. Compressibility Effects in Aerodynamics, Journal Aero. Sci. Volume 8, No. 9 (1941).

6. Tsien, H.S. two dimensional subsonic flow of compressible fluids. Journal Aero. Sci. Volume 6. No. 10 (1939).

7. Katsanis, T., and McNally, W.D., 'Fortran Program for calculating velocities and streamlines on the hub-shroud mid channel flow surface of an axial-or mixed flow turbo-machine, I-User's Mannual, NASA TND - 7343 (1973).

8. Bindon, J.P. and Carmichael A.D. streamline curvatures analysis of compressible and high mach number cascade flows. J. Mech. Engg. Sci. vol. 13, No. 5, pp. 344-357 (1971).

9. Wilkinson, D.H. Calculation of Blade-to Blade flow in a turbomachine by streamline curvature. Aero. Research Council R.& M. 3704 (1970).

10. Smith & Katsanis, "A Digital computer program for the subsonic flow past turbomachine blade using a matrix method. R&M No.3838.

11. Marsh, H., and Merryweather, H., The calculation of subsonic and supersonic flows in nozzles," cambridge University CUED/A-TURBO/TR 3, 1969.

12. Daneshyar, H., and Glynn, D.R., "The calculation of flow in nozzle using a time marching technique based on the method of charactersitic," Cambridge University CUED/A-Turbo/TR 33, 1972.

13. Gopalakrishnan, S., and Bozzola, R., "Computation of shocked flow in compressor cascade, " ASME Paper No. 72-GT-31.

14. McDonald, P.W., "The computation of transonic flow through Two-dimensional Gas turbines cascade, " ASME Paper No. 71-GT-89-1971.

15. Akay, H.U., Ecer, A., "Transonic flow computations in cascade using finite element method.

16. Thompson D.S. "Finite Element analysis of the flow through a cascade of Aerofoils', Aero. Research Council Report No. 34, 412 (1973).

17. Smith, L.H., Jr., 'The radial equilibrium equation of Turbomachinery, J. of Engg. for Power, Jan. 1966.

18. Novak, R.A., 'Streamline Curvature computing procedures for fluid flow problems', J. of Engg. for Power, Oct., 1967.

19. Novak, R.A., and Hearsey, R.M., 'A nearly three dimensional computing system for turbomachinery, Part I and II', ASME Paper No. 76-FE-20 March, 1976.

20. Frost, D.H., 'A streamline curvature through flow computer program for analysing the flow through axial flow turbomachines, Aeronautical Research Council, R. and M. 3687, August, 1970.

21. Carter, A.F., Platt, M., and Lenherr, F.K., 'Analysis of geometry and design point performance of axial flow turbines Part I-Development of the analysis method and loss coefficient Correlation, NASA CR 1181, Sept., 1968.

22. Horlock, J.H., 'Axial flow turbines', Butter Worths Pub., 1966.

23. Ainley, D.G. Mathieson, G.C.R. "A Method of performance estimation for axial flow turbines", H.M.S.O., A.R.C., R. & M. 2974, 1957.

24. Dunham, J., Came, P.M. "Improvements to the Ainley-Mathieson Method of turbine performance prediction", Am. Soc. Mech. Engrs. Paper 70-GT-2, 1970.

25. Kacker, S.C., Okapuu, U., "A mean line prediction method of axial flow turbine efficiency", Am. Soc. Mech. Engrs. Paper 81-GT-58, (1981 May).

26. Smith, S.F., "A simple correlation of turbine efficiency" J. Royal Aero. Soc., Volume, 69, July, 1965.

27. Balje, O.E., Binsley R.L., 'Axial turbine performance evaluation loss geometry relationship Part A, J. of Engg. for Power,October, 1968.

28. Hirsch, Ch., and Warzee, G., 'A finite element method for the axisymmetric flow computation in a turbomachine', Int. J. for Numerical Methods in Engg., Volume, 10, 1976.

29. Davis, W.R., and Millar, D.A.J. 'A comparison of the matrix and streamline curvature method of axial flow turbomachinery analysis, From a user's point of view, J. of Engg. for Power, Oct., 1975.

30. Denton, J.D. Through flow calculations for transonic axial flow turbines CEGB Laboratory Report.

31. Kofskey, M.G., Roelke, J.R., and Haas, E.J., 'Turbine for low cost turbojet engine, Part II-opened stator', NASA TND - 7625.

32. Evans, D.C., and Hill, J.M., 'Experimental investigation of a 4½ stage turbine with very high stage loading factor, I-turbine design, NASA CR - 2140, 1973.

33. Walker, N.D. and Thomas, M.W., 'Experimental investigation of a 4½- stage turbine with very high loading factor, II-turbine performance', NASA CR-2363, 1974.

34. Wolfmeyer, G.W., and Thomas, M.W., 'Highly loaded multistage fan drive turbine-performance of initial seven configuration', NASA CR 2362, 1974.

35. Kofskey, M.G., and Nusbaum, W.J., 'Design and Cold-air investigation of a turbine for a small low-cost turbofan engine', NASA TND-6967.

36. Majumdar, A.S., 'A review of recent computational procedures for off-design analysis of axial compressors', J. of the Aero. Soc. of India, Vol. 27, No. 1 Feb., 1975.

37. Schlichting, H. and Scholz, N., Uber die theoretische Berechnung der Stromungsverluste eines ebenen Schaufelgitters. Ing.- Arch., Bd. XIX, Heft 1 (1951).

38. Daneshywar, 'A critical assessment of methods of calculating slope and curvature of streamlines in fluid flow problems', Proc. Inst. of Mech. Engg., Vol. 186, 70/72.

39. Govindan, T.R. 'A Computing System for the Design-Point Performance of Axial turbines, January, 1978.
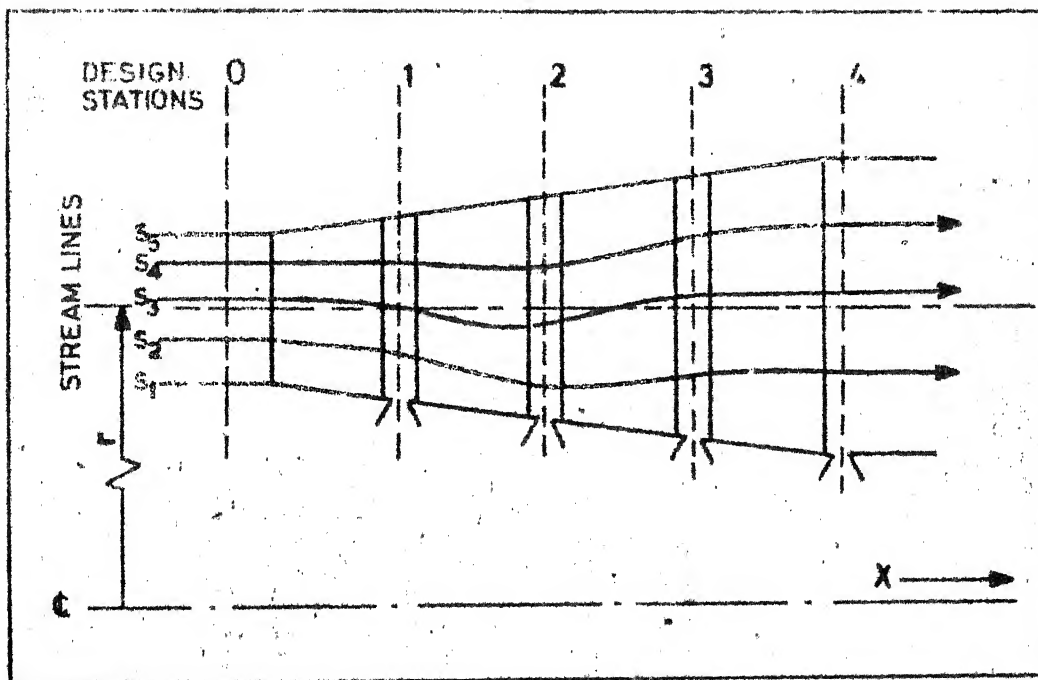
Fig. 1 Meridional section of a turbine.
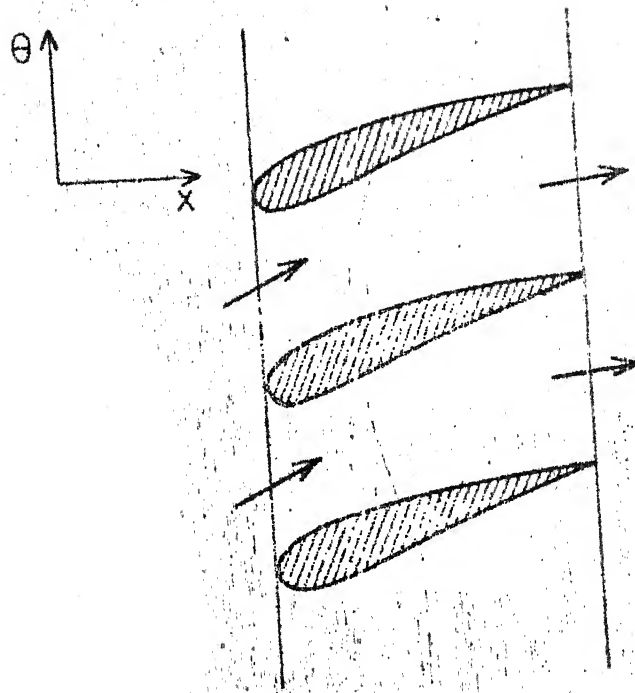
Fig 1 A Blade to blade section of a turbine
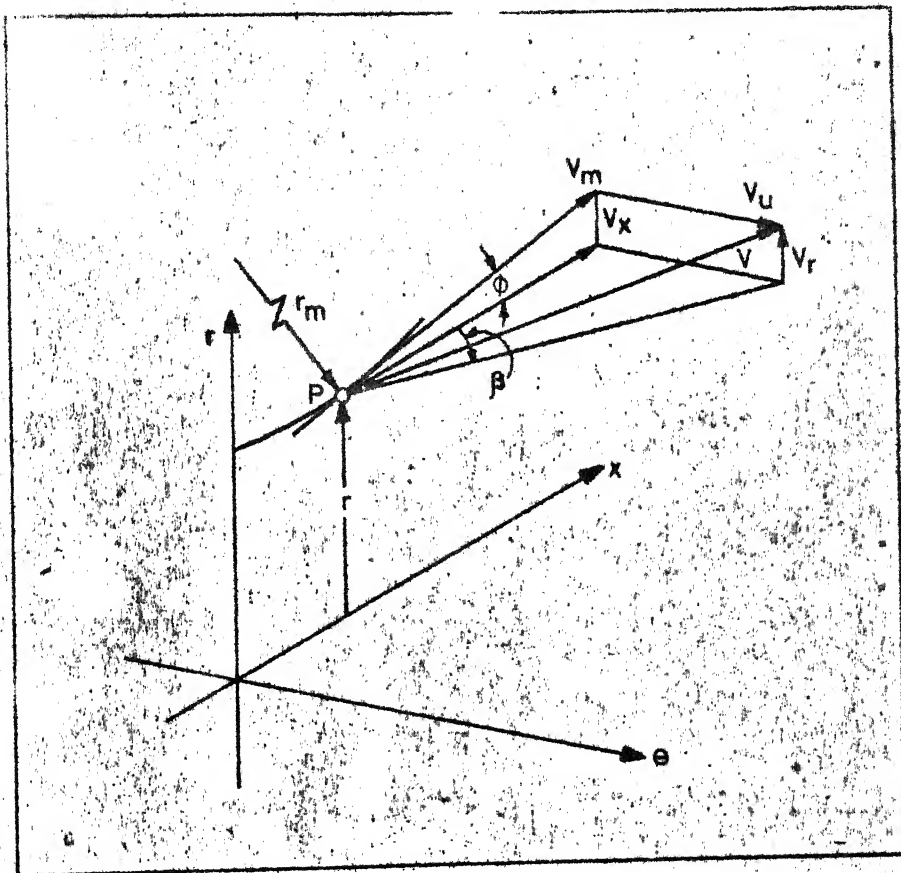
Fig. 2   Nomenclature for the flow

Fig. 3   Enthalpy-entropy diagram for a stage
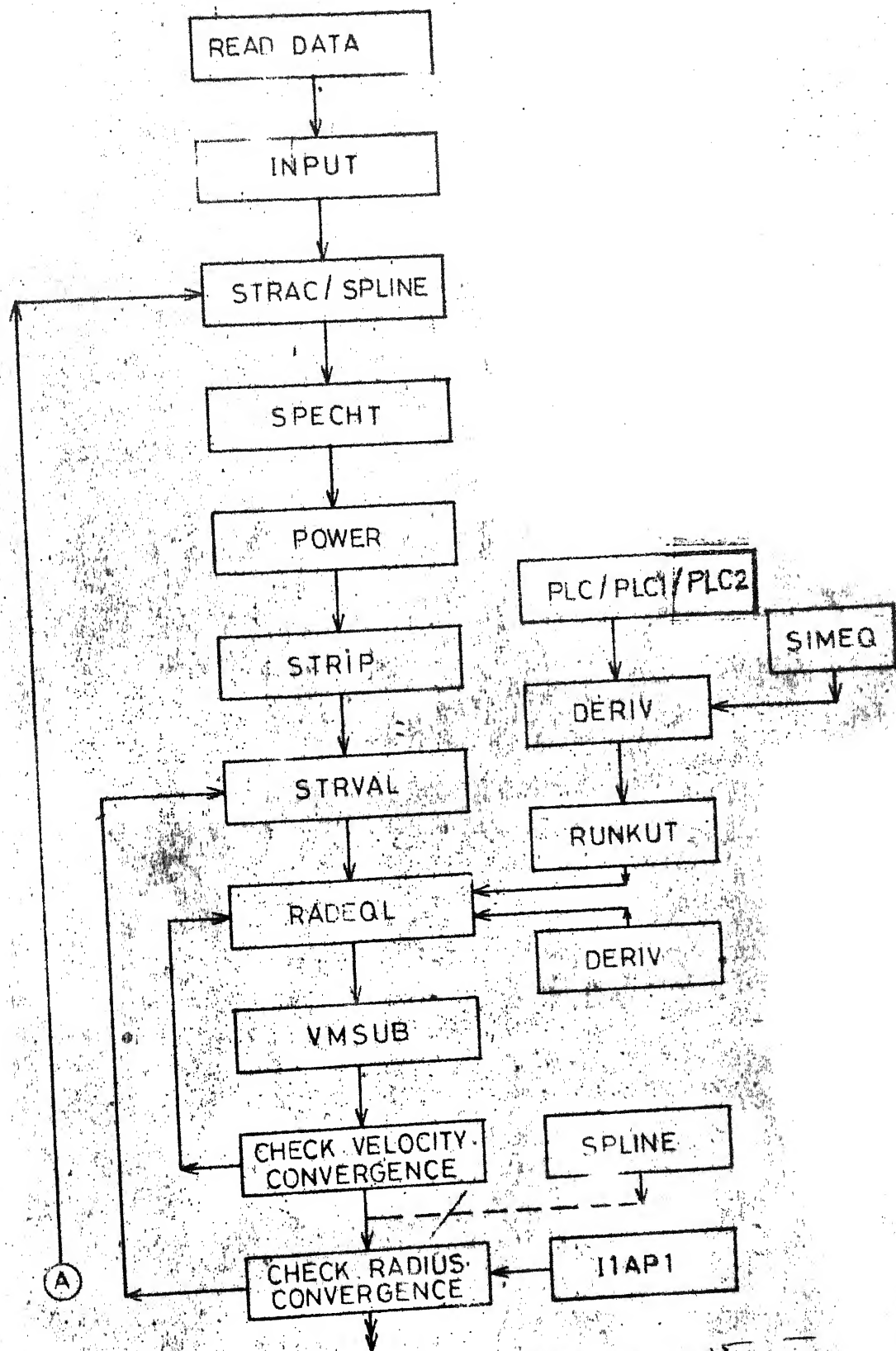
Fig . 4 ---- (Continued)
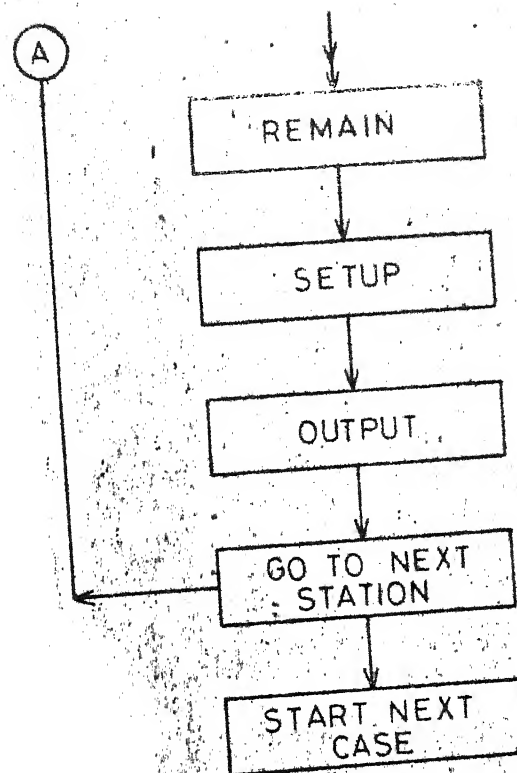
Fig 4   Flow chart of subroutine calling sequence
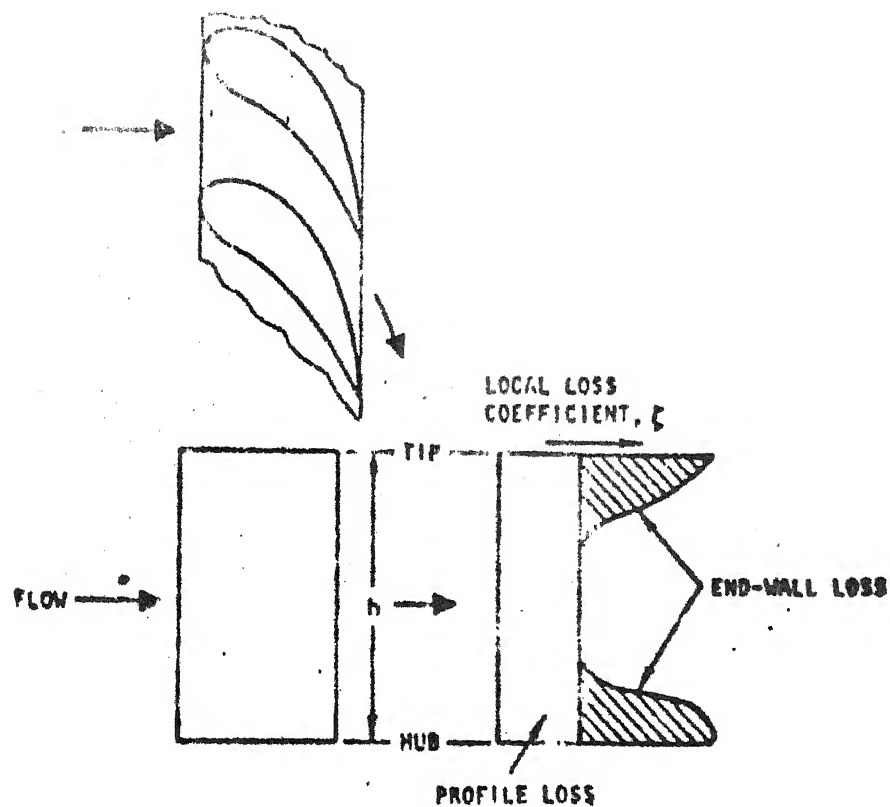
Fig. 5 Loss model
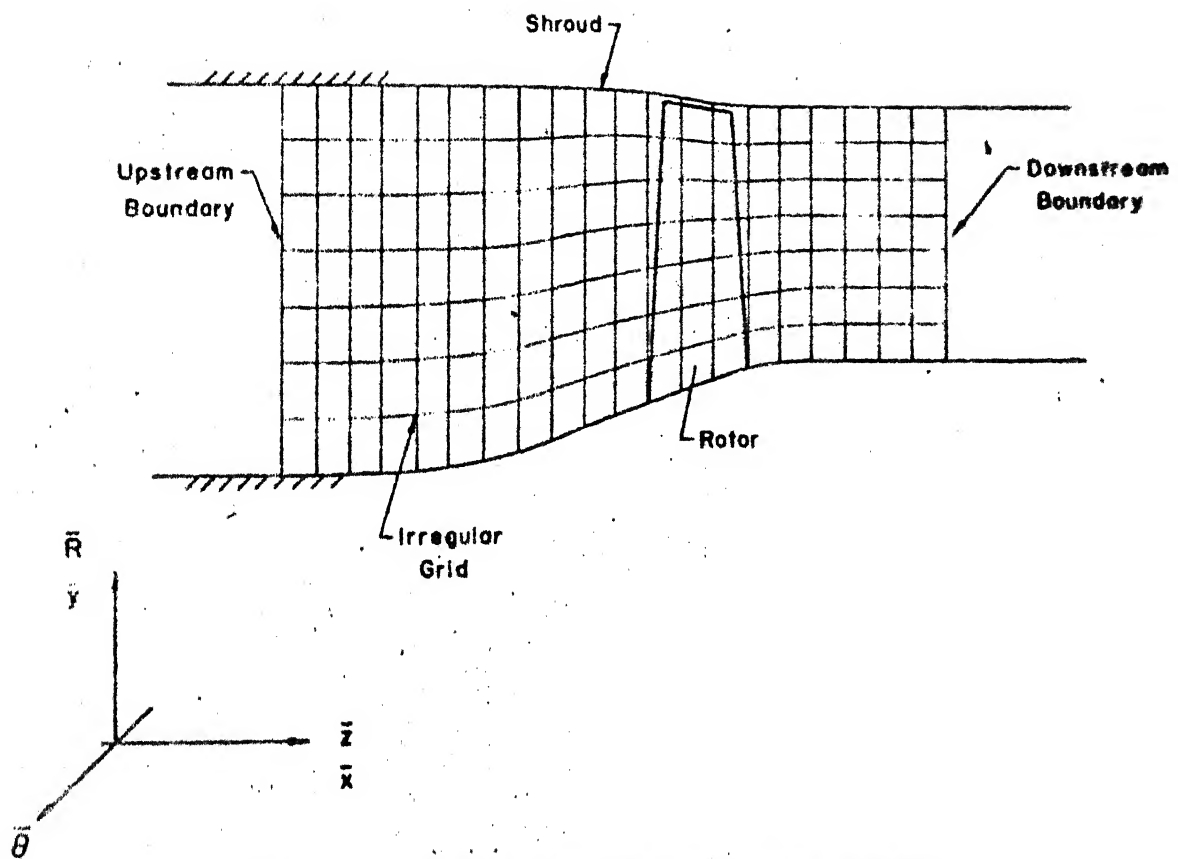
Fig. 5 A   Matrix grid and coordinate system
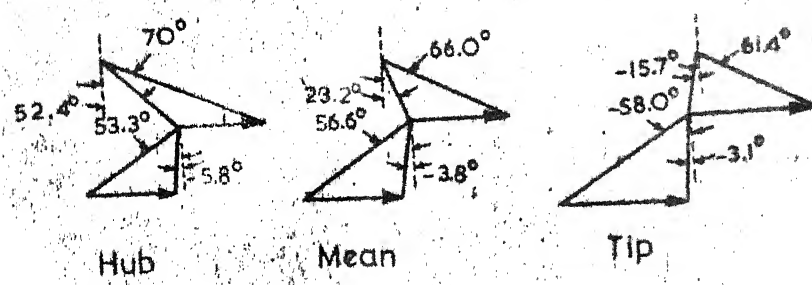
DESIGN VELOCITY DIAGRAMS
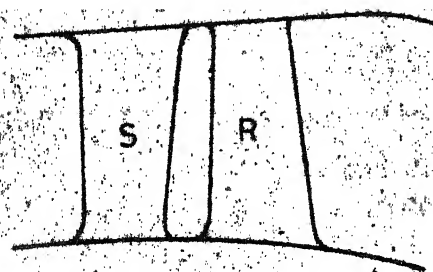
TURBINE FLOWPATH

Fig. 6 (Test case 1)
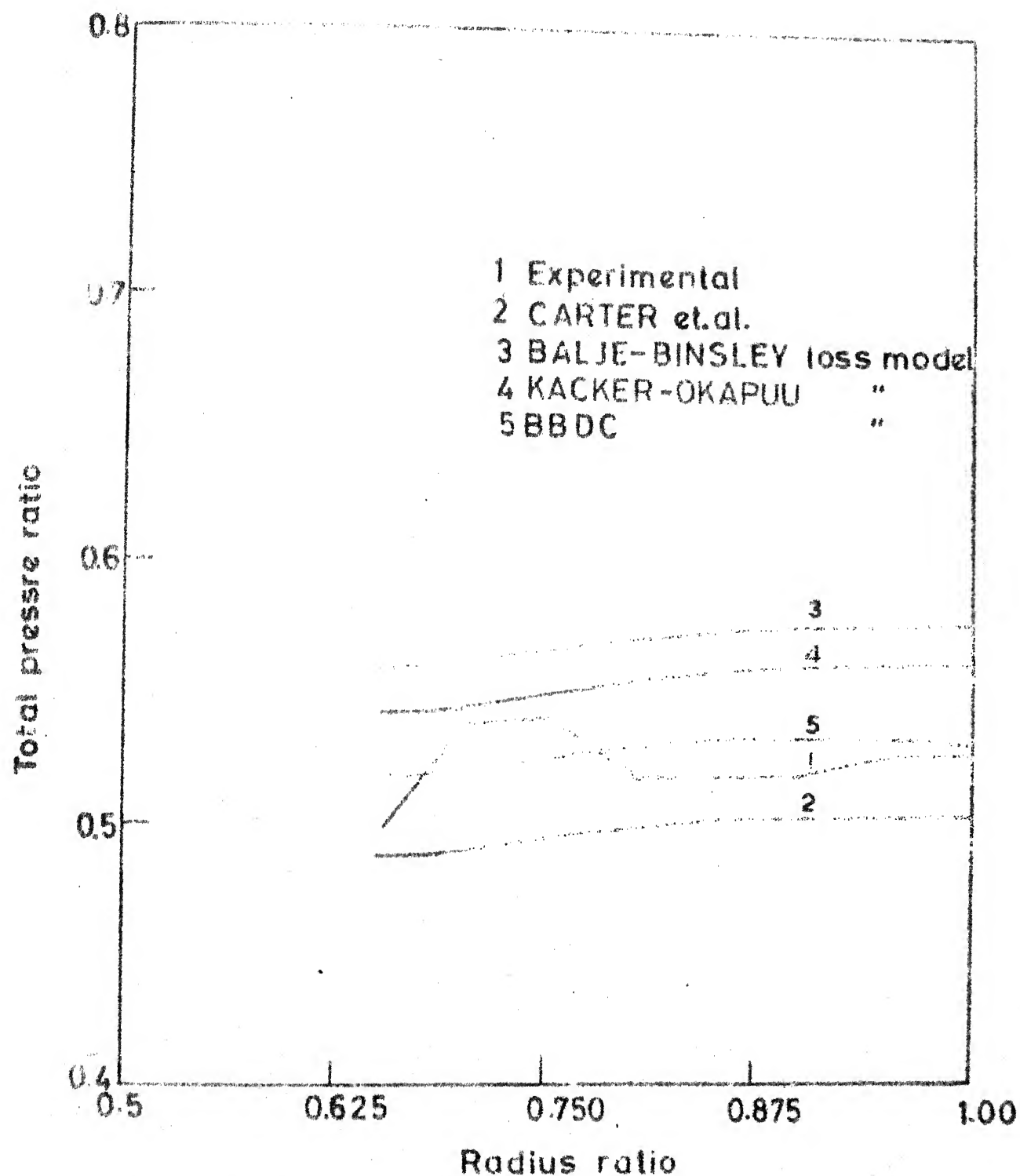
FIG.7 STAGE EXIT TOTAL PRESSURE DISTRIBUTION FOR TEST CASE I
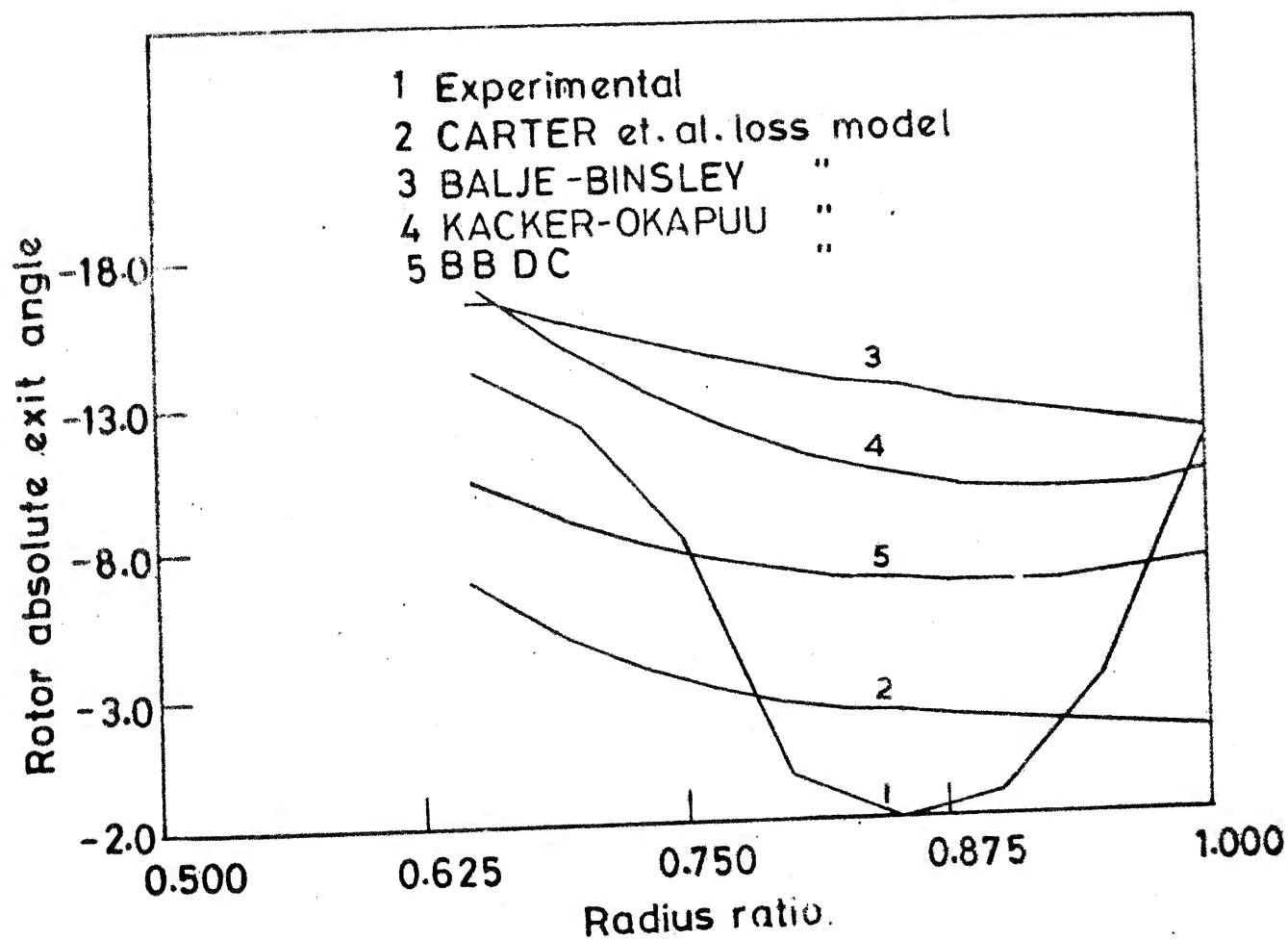
FIG.8 OUTLET FLOW ANGLE DISTRIBUTION AT TURBINE EXIT FOR TEST CASE -I
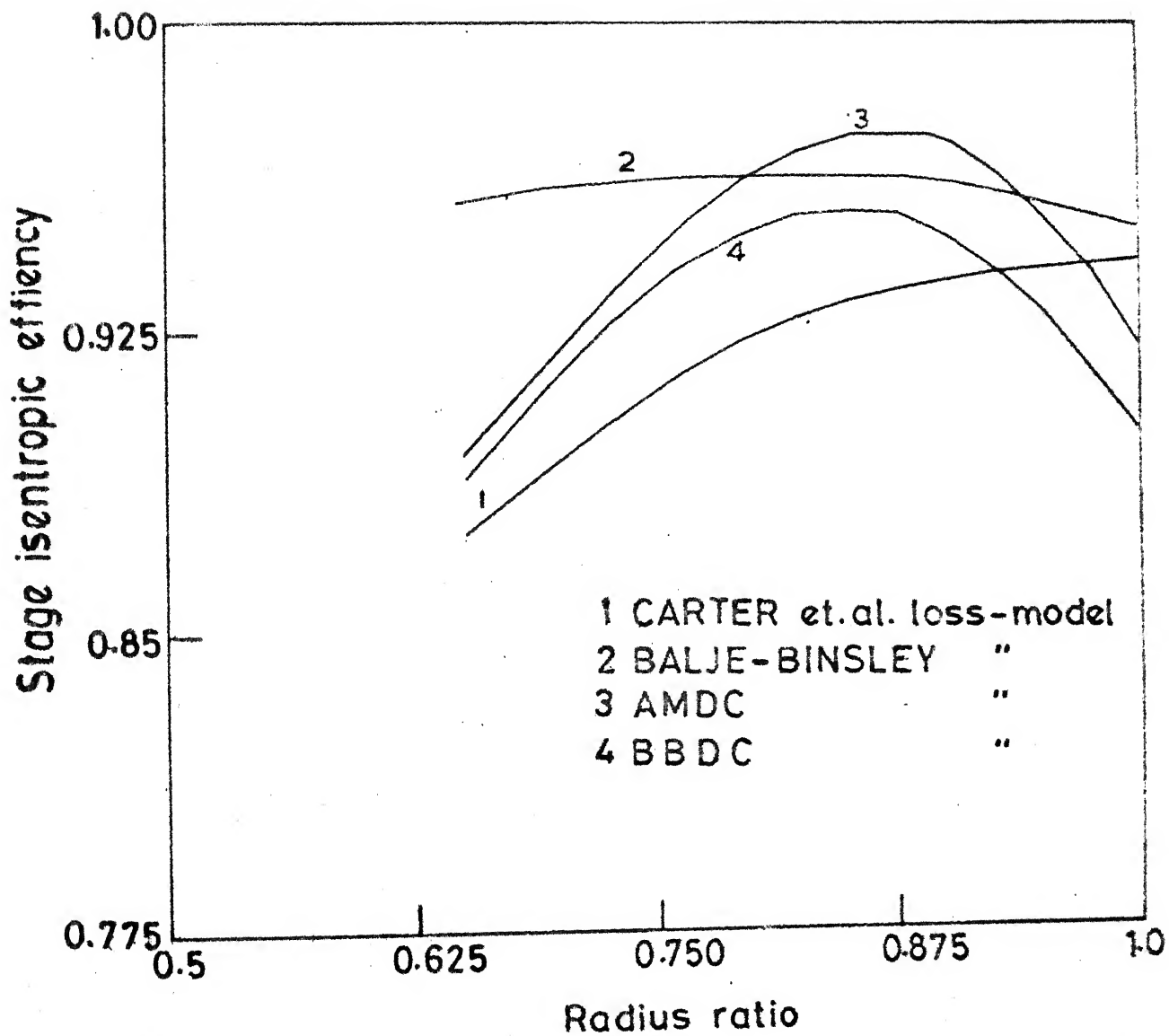
FIG.9 RADIAL DISTRIBUTION OF TOTAL TO TOTAL EFFICIENCY FOR TEST CASE I
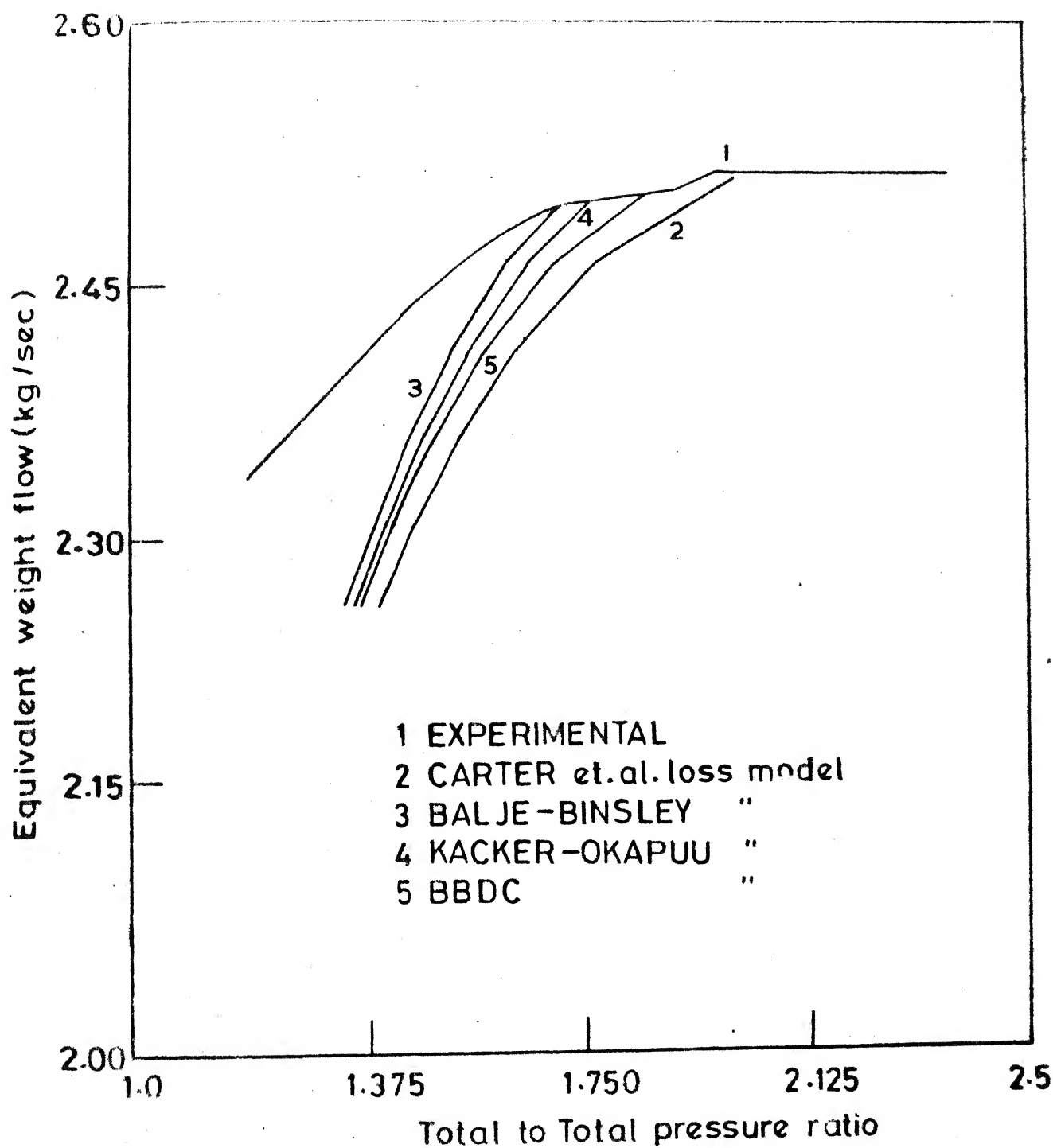
FIG. 10 EQUIVALENT WEIGHT FLOW VS TOTAL TO TOTAL PRESSURE RATIO FOR TEST CASE-1
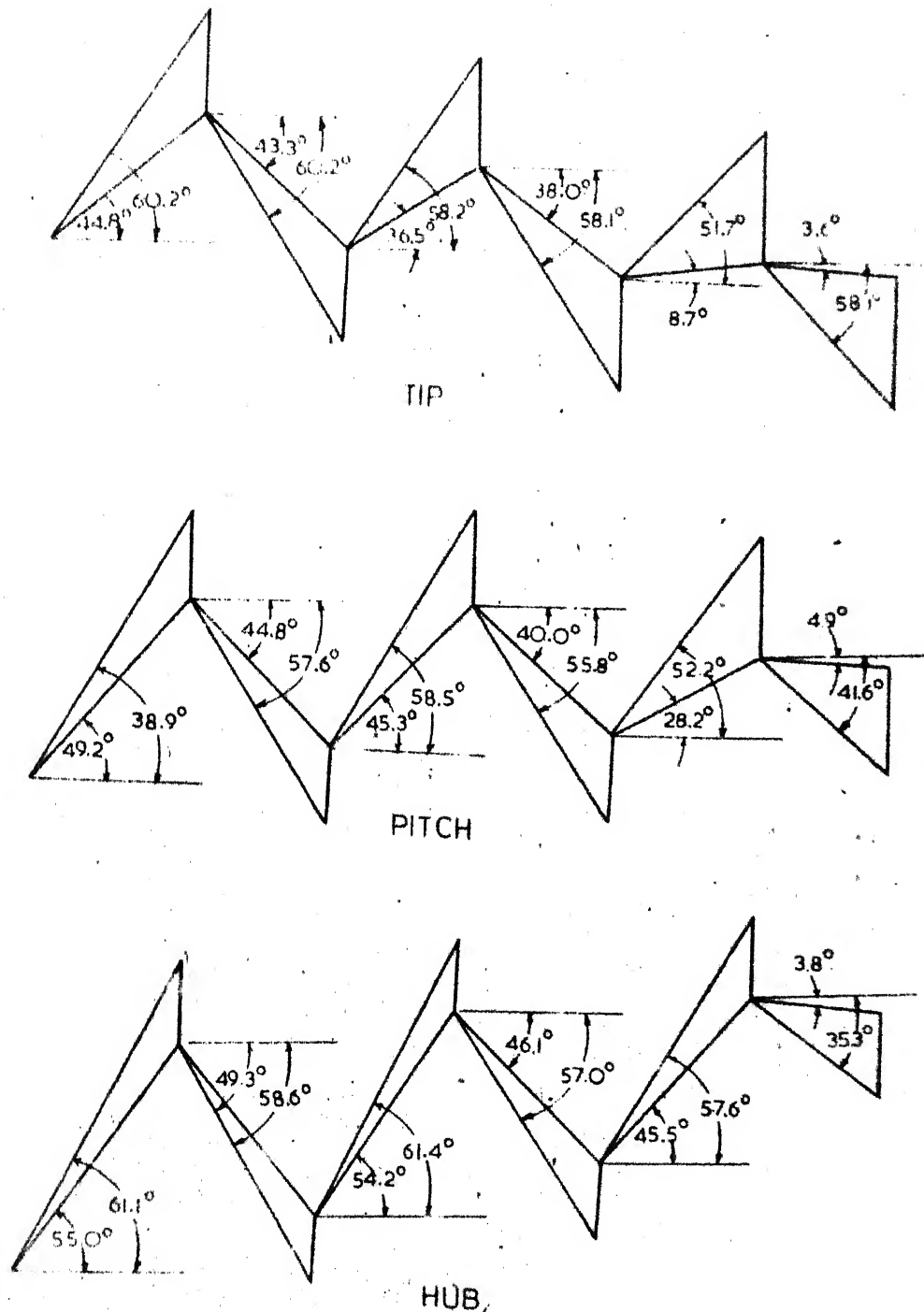
Fig. 11: Turbine design velocity diagrams
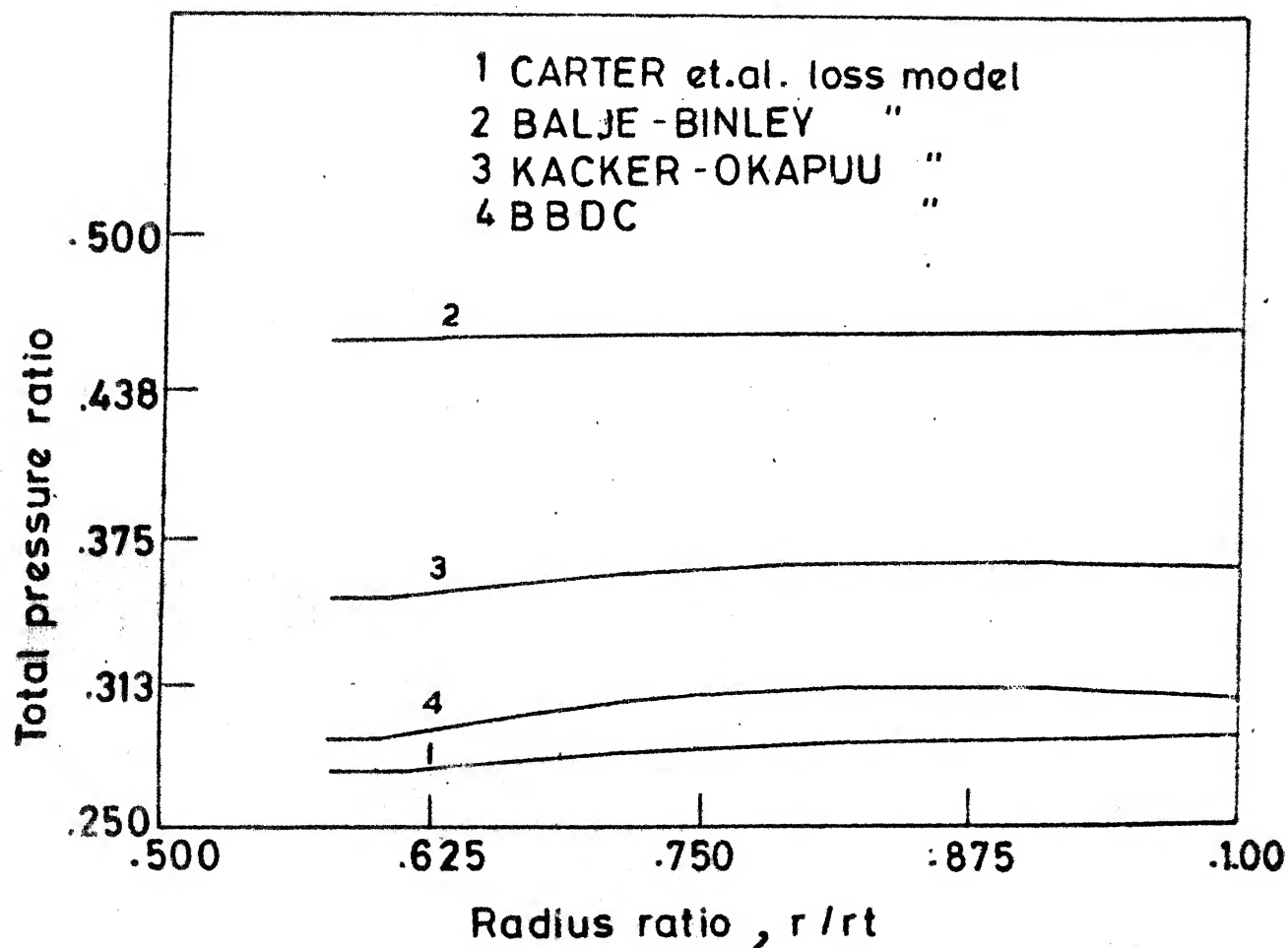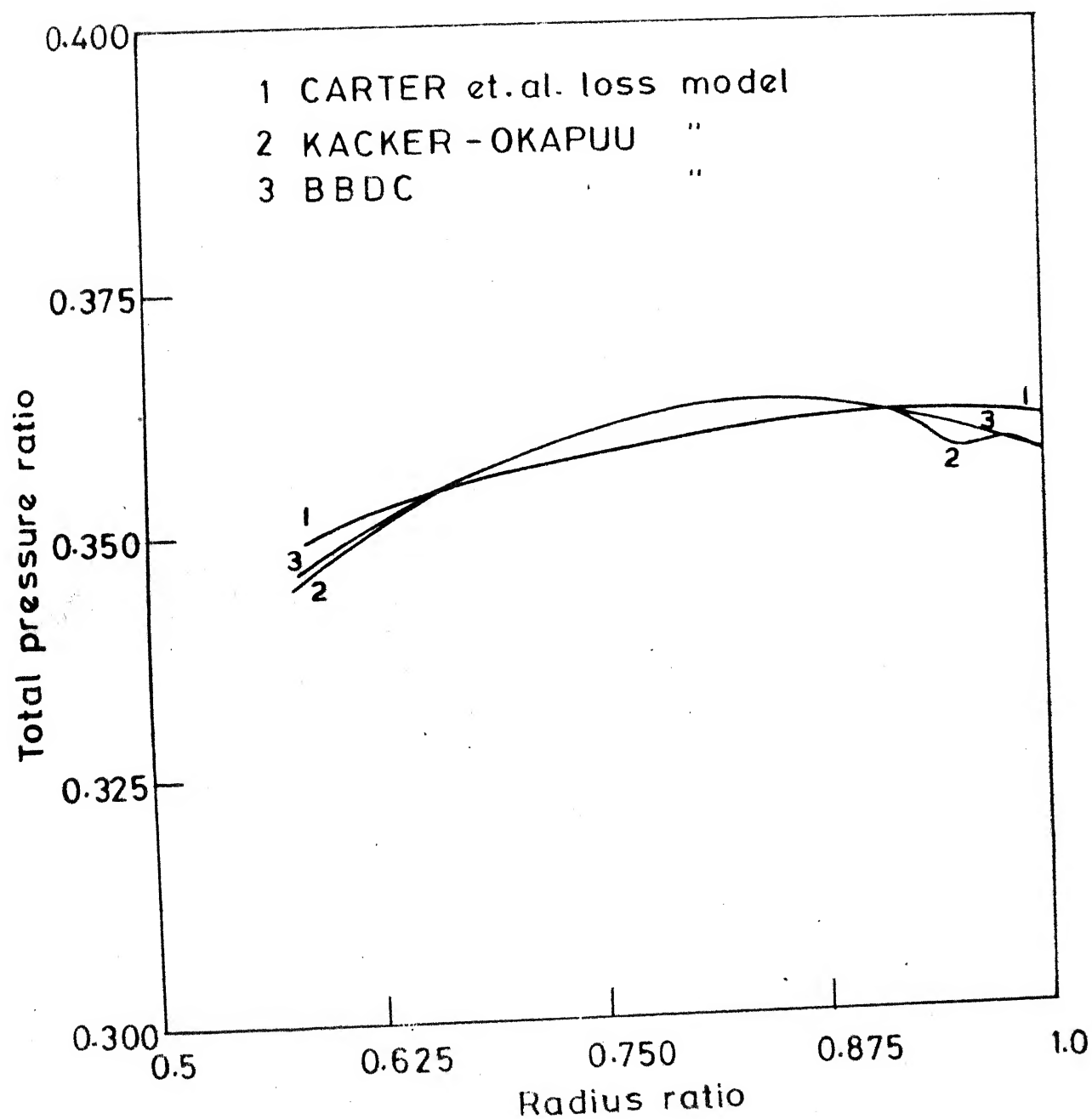(test case 2)
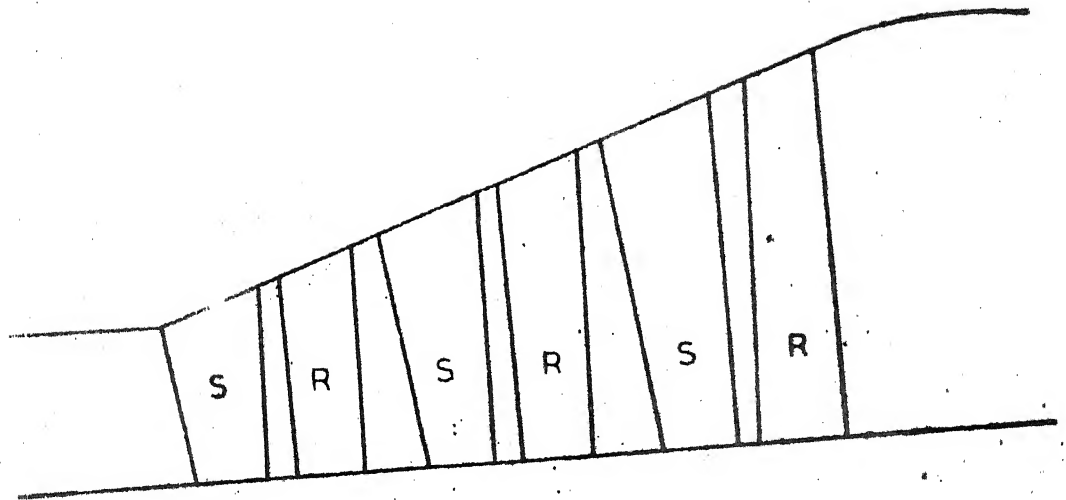
Fig. 12   Turbine flowpath (Test case 2)

1.0

.813

Static pressure / inlet total pressure

.625

.438

.250

4   3
2   1

1   Experimental at Hub
2   "   " Tip
3   CARTER et al loss model
    at Hub
4   CARTER   "   "
    at Tip

0   .75   1.1   1.3   1.5 1.7   2.25   3.0

Axial stations
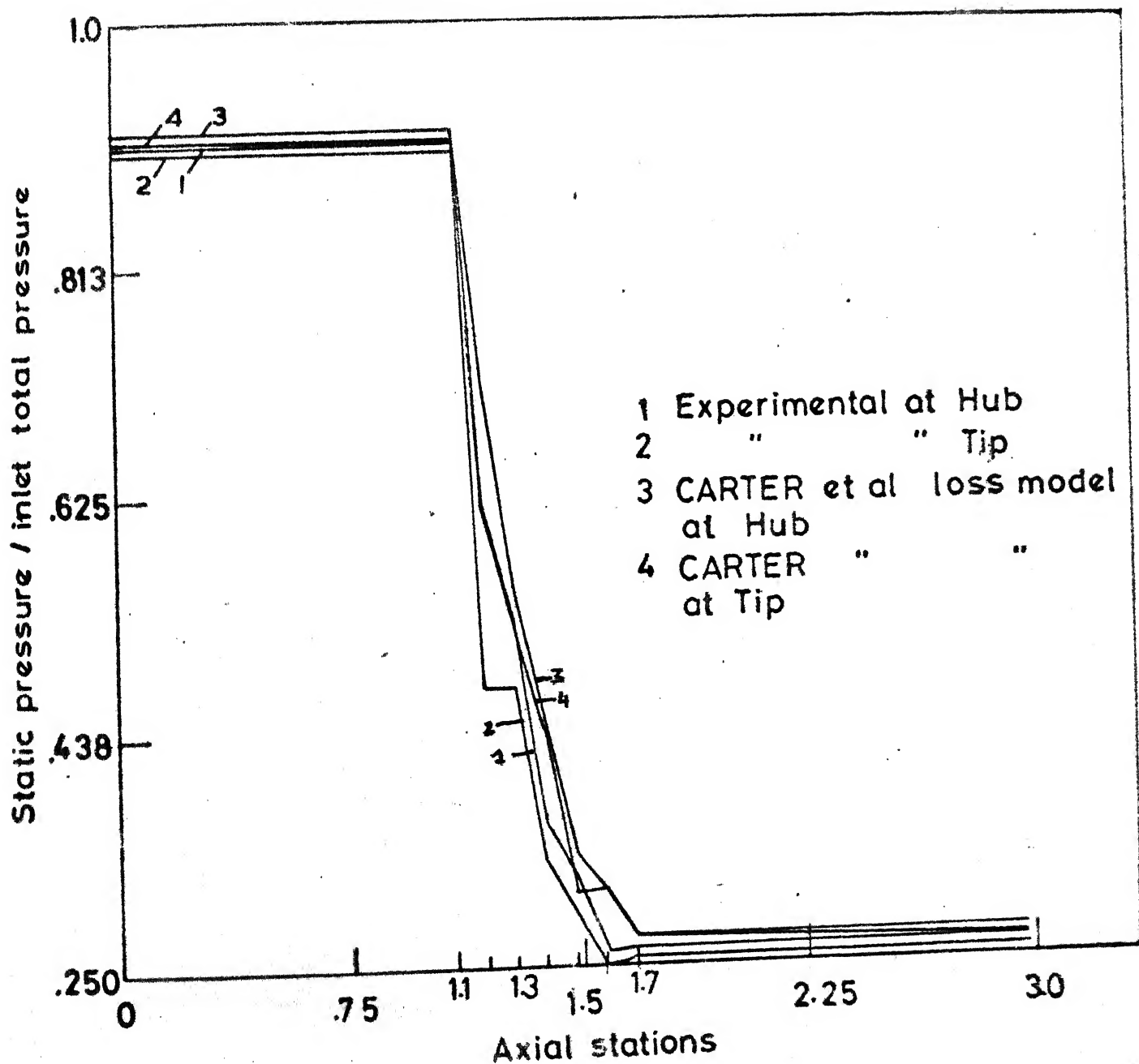
FIG.13 HUB AND TIP STATIC PRESSURE DISTRIBUTION FO
TEST CASE No.2
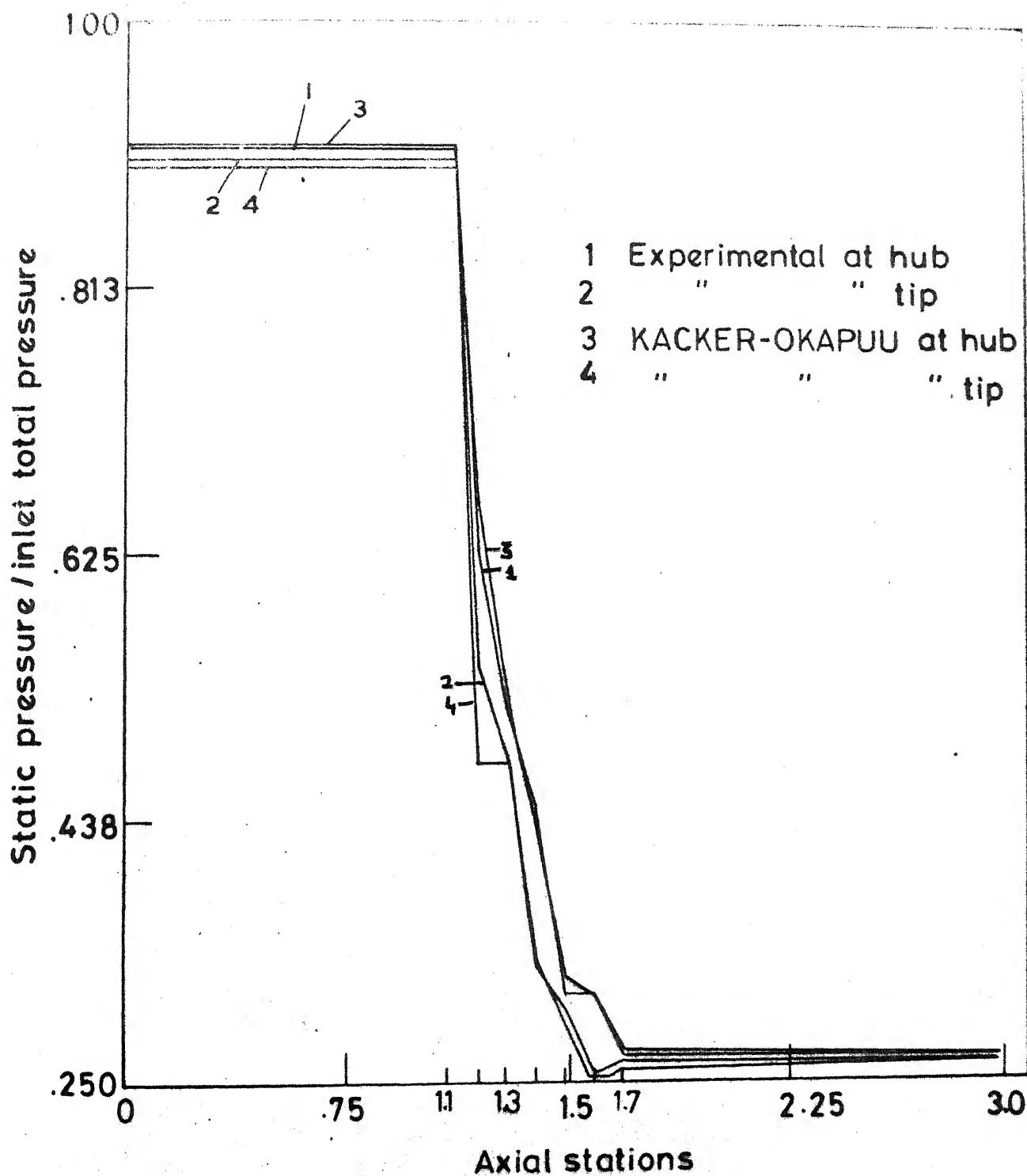
FIG.14 HUB AND TIP STATIC PRESSURE DISTRIBUTION FOR TEST CASE No.2
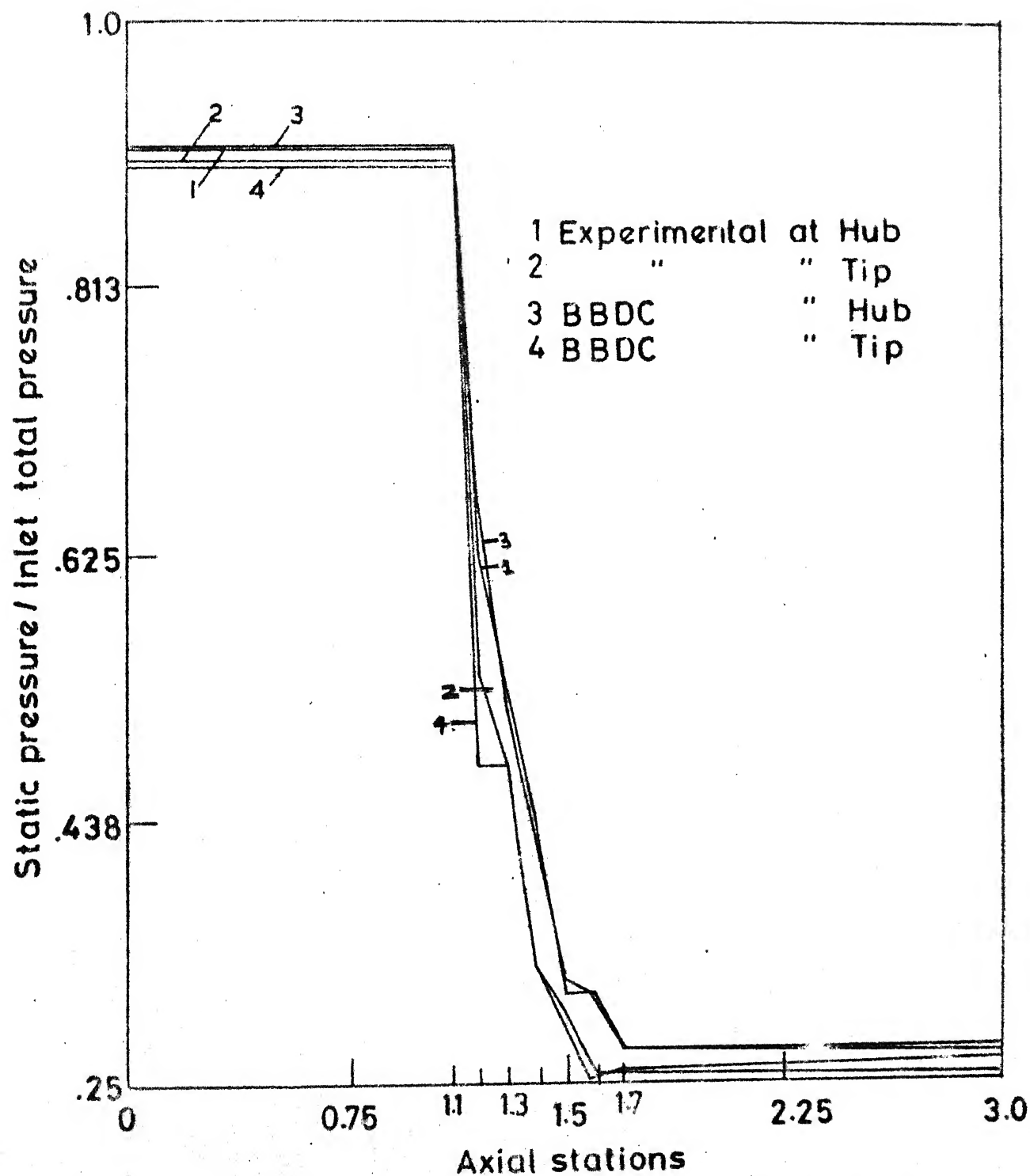
FIG.15 HUB ANDTIP STATIC PRESSURE DISTRIBUTION
FOR TEST CASE No. 2
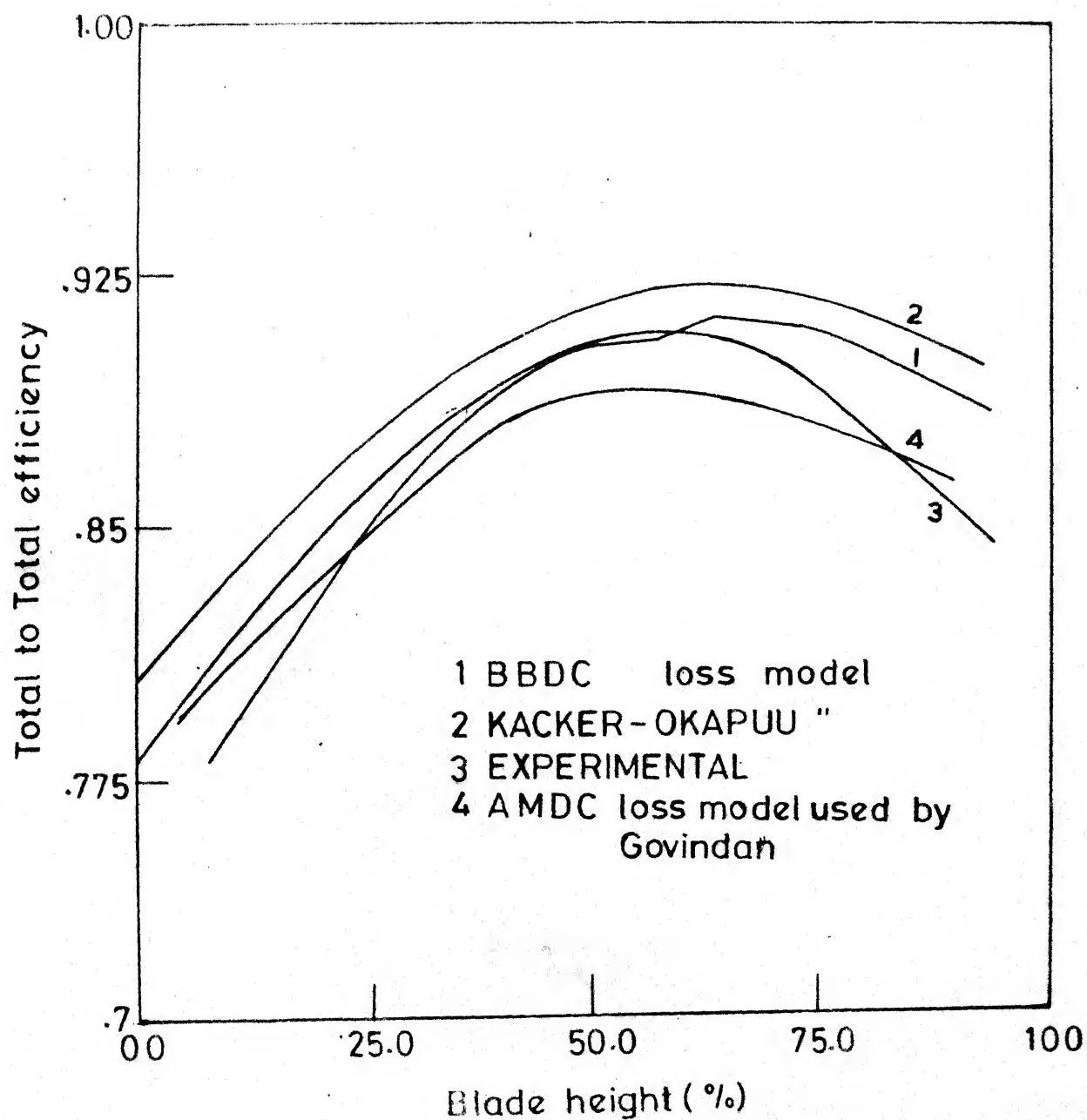
FIG. 16 TOTAL TO TOTAL EFFICIENCY DISTRIBUTION
AT STAGE 2 EXIT FOR TEST CASE 2
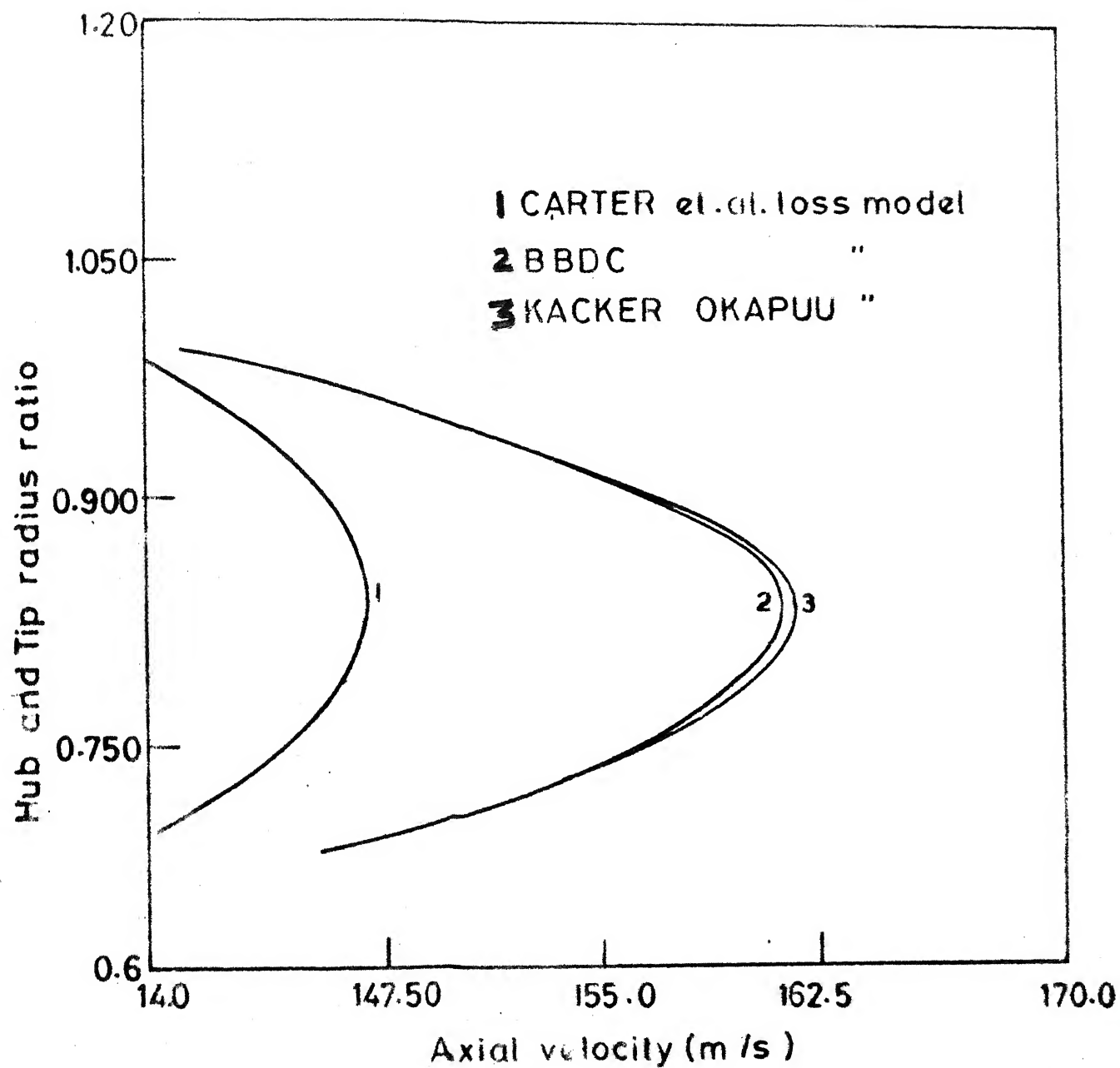
FIG. 17   AXIAL VELOCITY DISTRIBUTION AT ENTRY TO
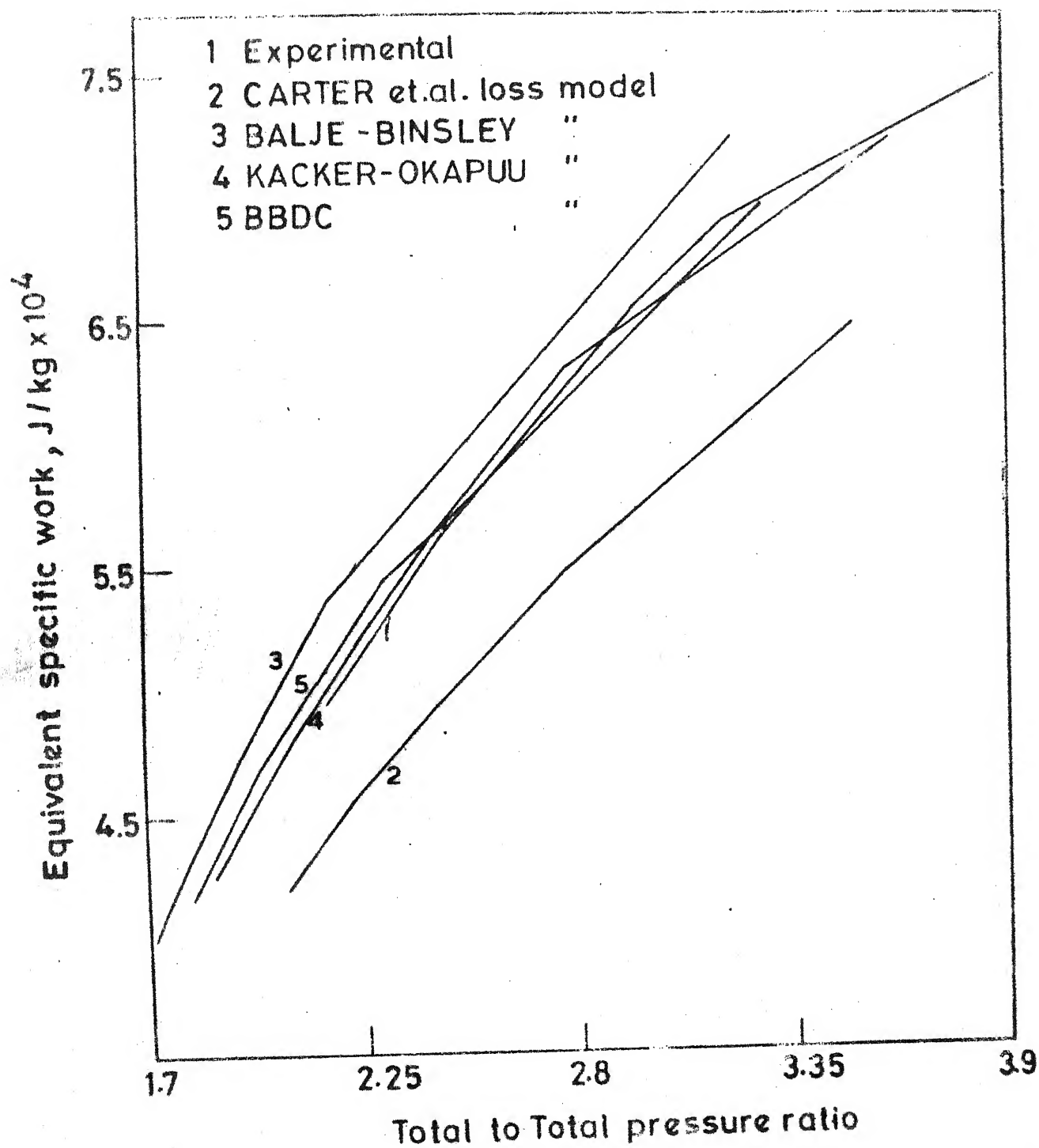THE LAST STAGE OF TURBINE FOR TEST
CASE 2
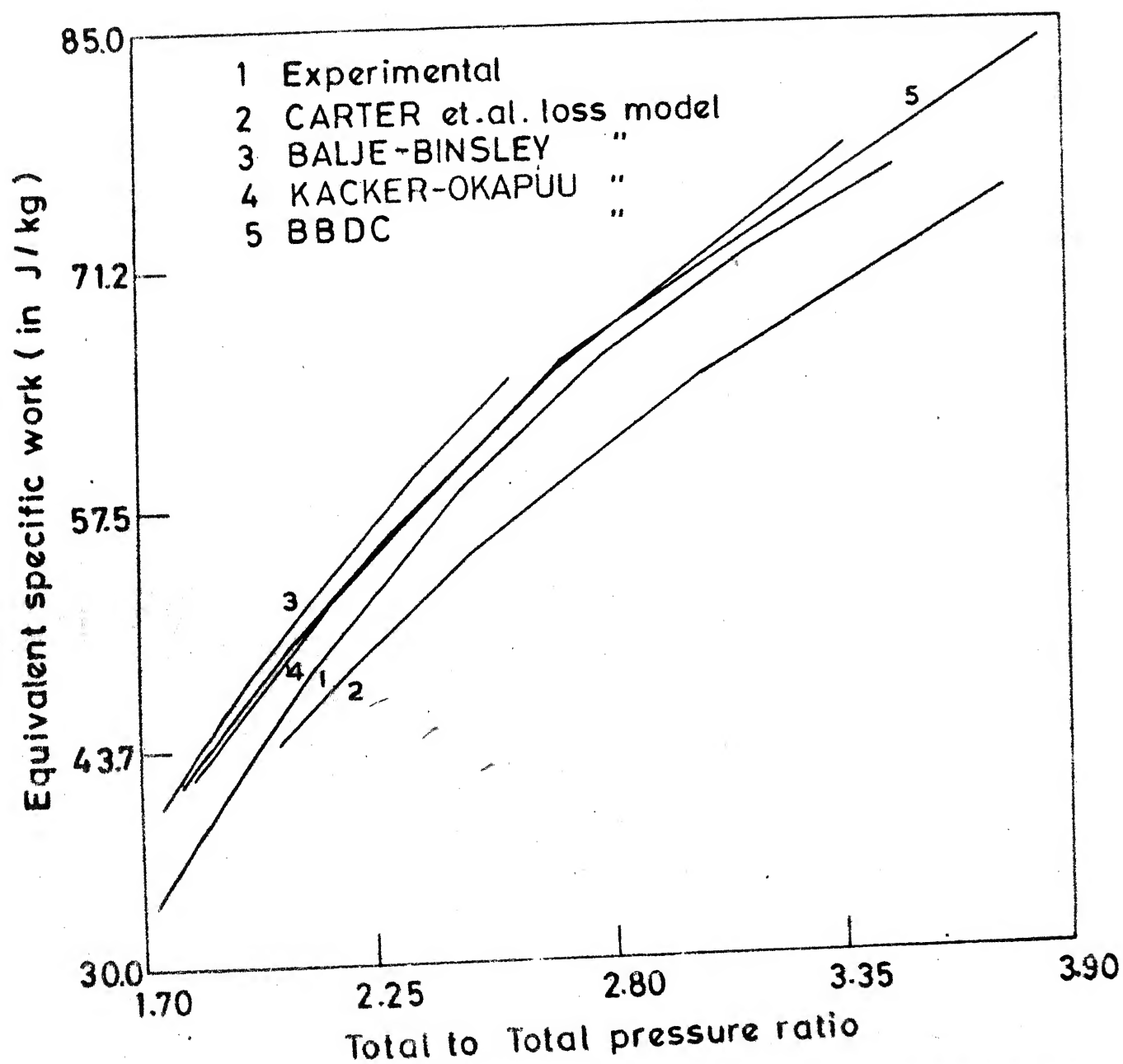
FIG.18. EQUIVALENT SPECIFIC WORK VS TOTAL TO TOTAL PRESSURE RATIO FOR TEST CASE No
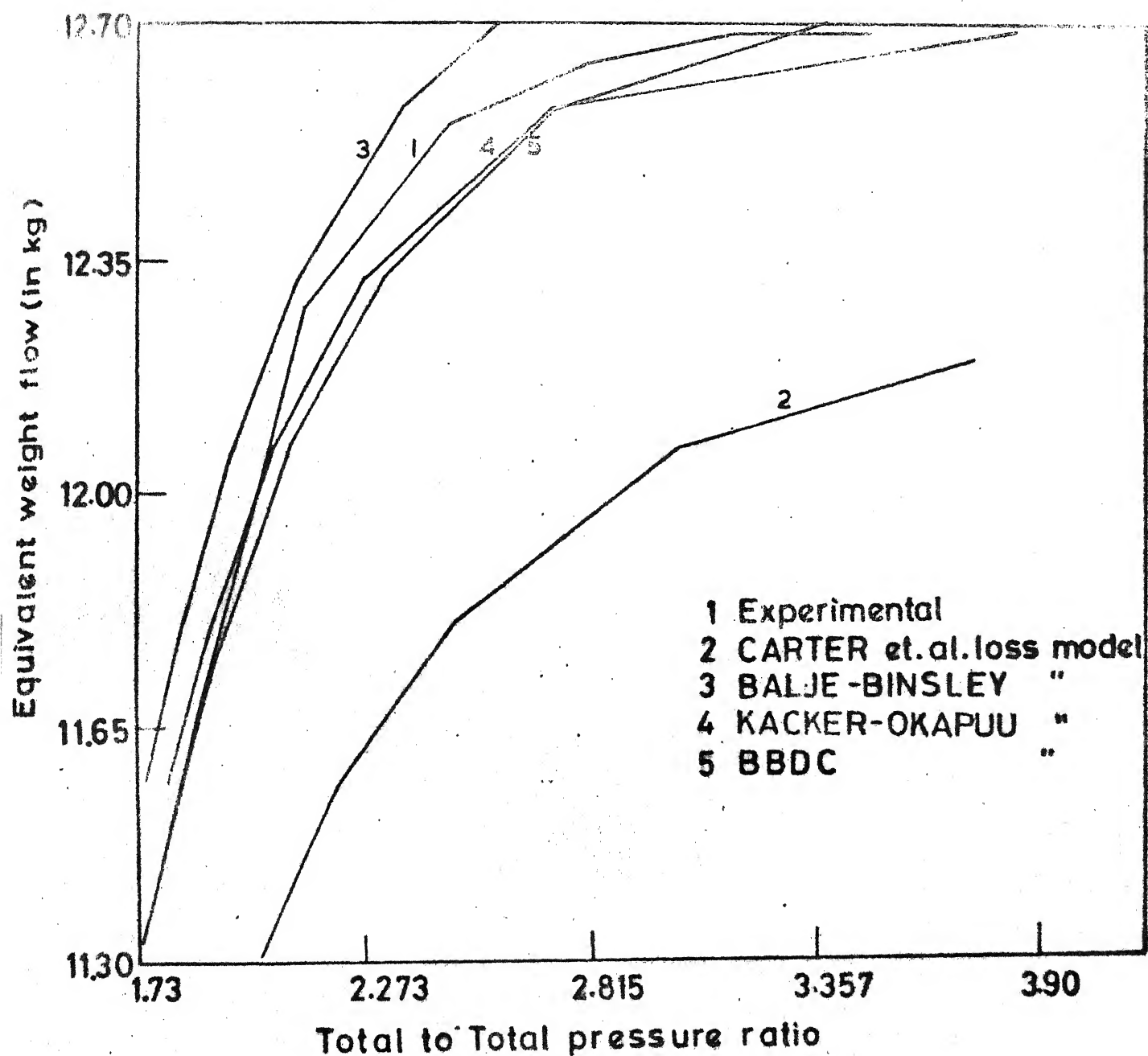
FIG.19 EQUIVALENT WEIGHT FLOW VS TOTAL TO TOTAL PRESSURE RATIO FOR TEST CASE NO. 2
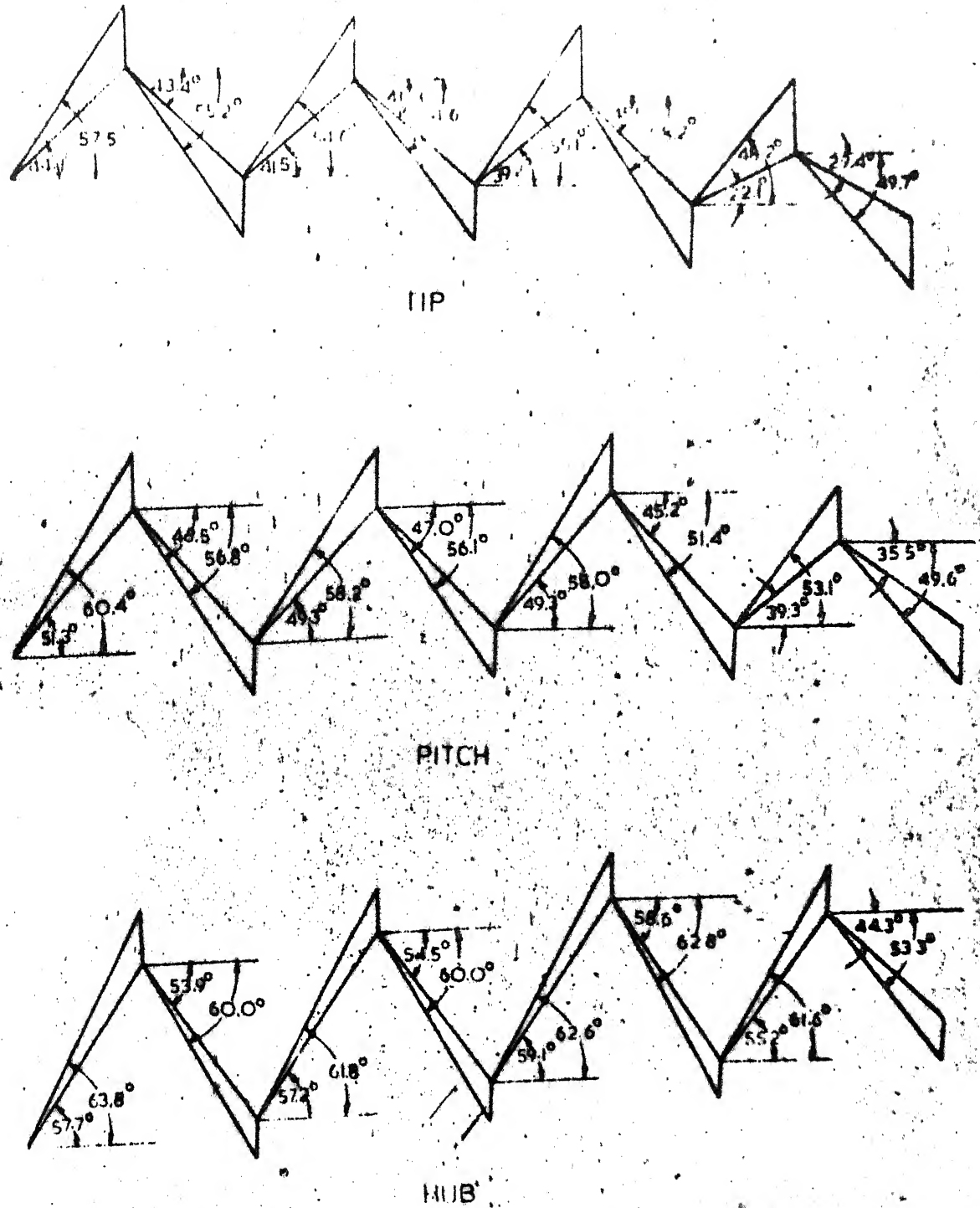
Fig. 20 Turbine design velocity diagrams (test case)
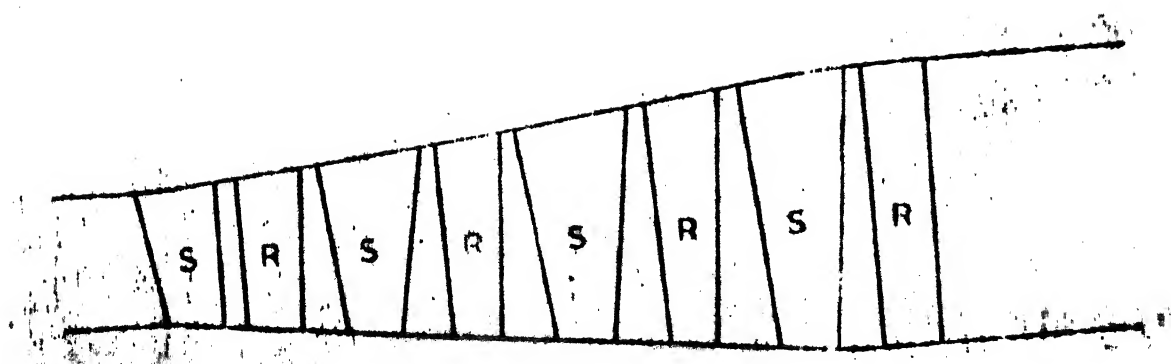
Fig. 21 Turbine flowpath (Test case 3)

FIG. 22 STAGE EXIT TOTAL PRESSURE DISTRIBUTION FOR TEST CASE 3 -DESIGN MASS FLOW RATE

FIG. 23 STAGE EXIT TOTAL PRESSURE DISTRIBUTION FOR TEST CASE 3
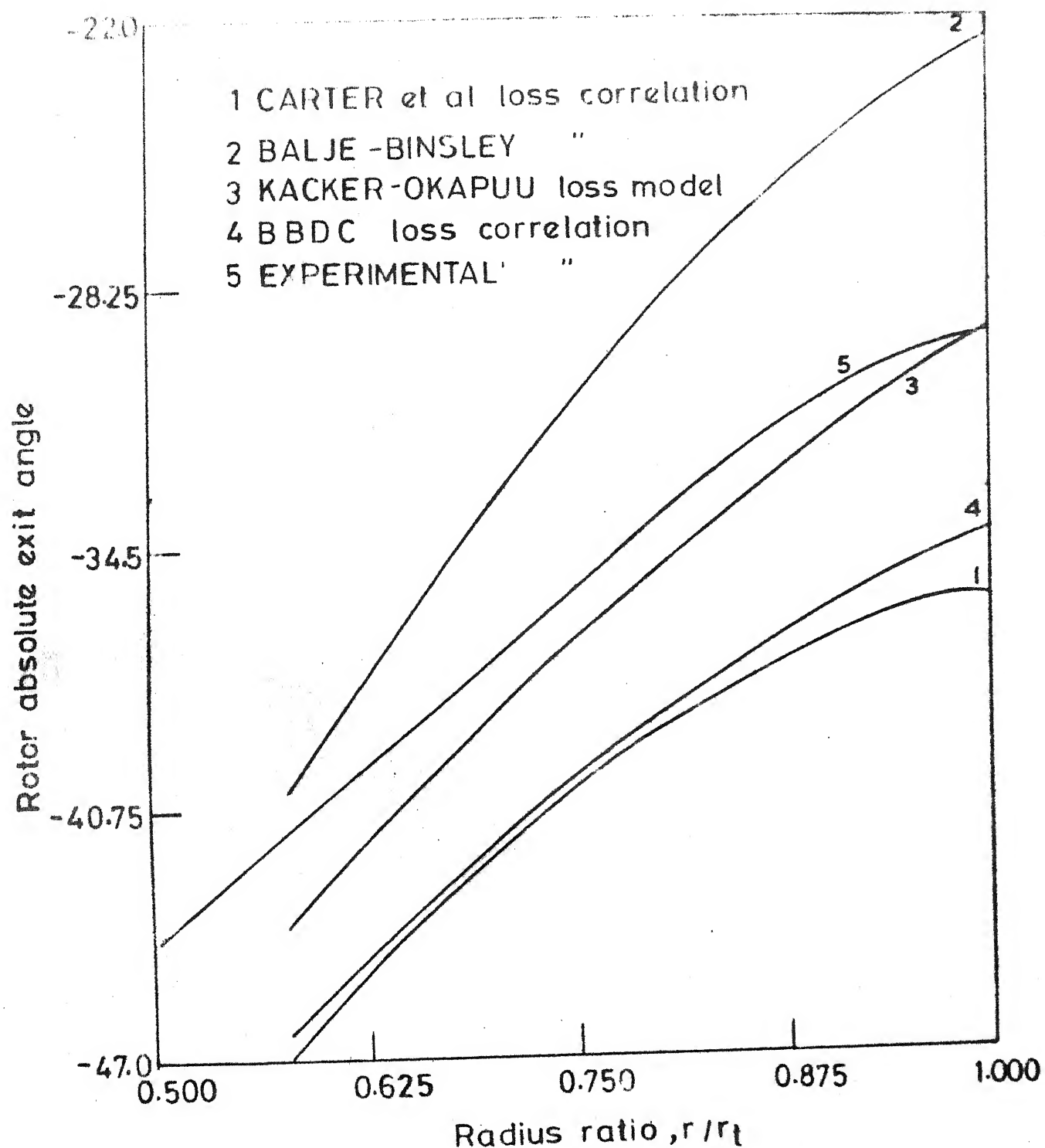
FIG. 24 OUTLET FLOW ANGLE DISTRIBUTION AT TURBINE EXIT FOR TEST CASE 3

FIG.25 EQUIVALENT SPECIFIC WORK VS TOTAL TO TOTAL PRESSURE RATIO FOR TEST CASE No. 2
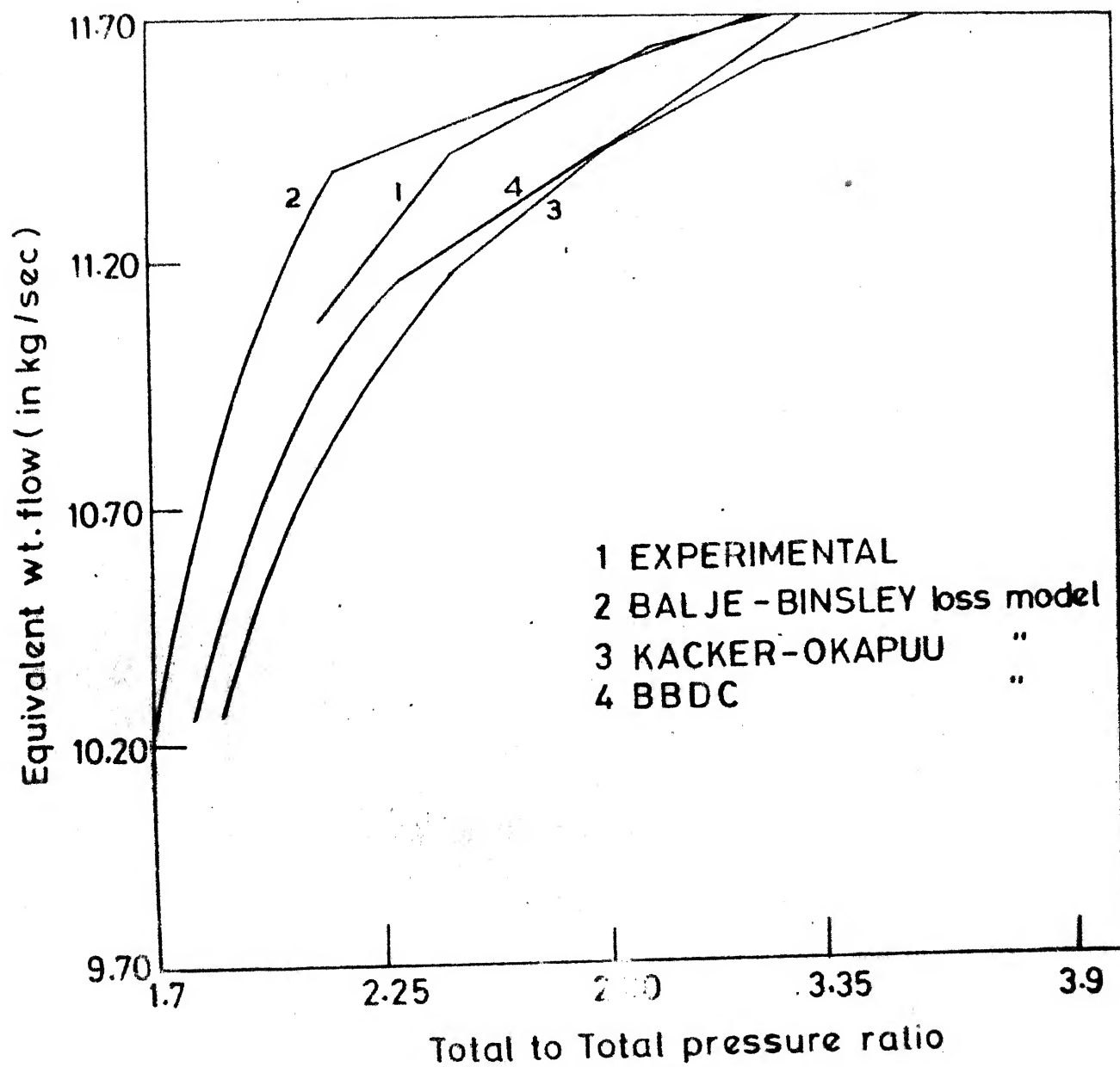
FIG. 26 EQUIVALENT WEIGHT FLOW VS TOTAL TO TOTAL PRESSURE RATIO FOR TEST CASE 3
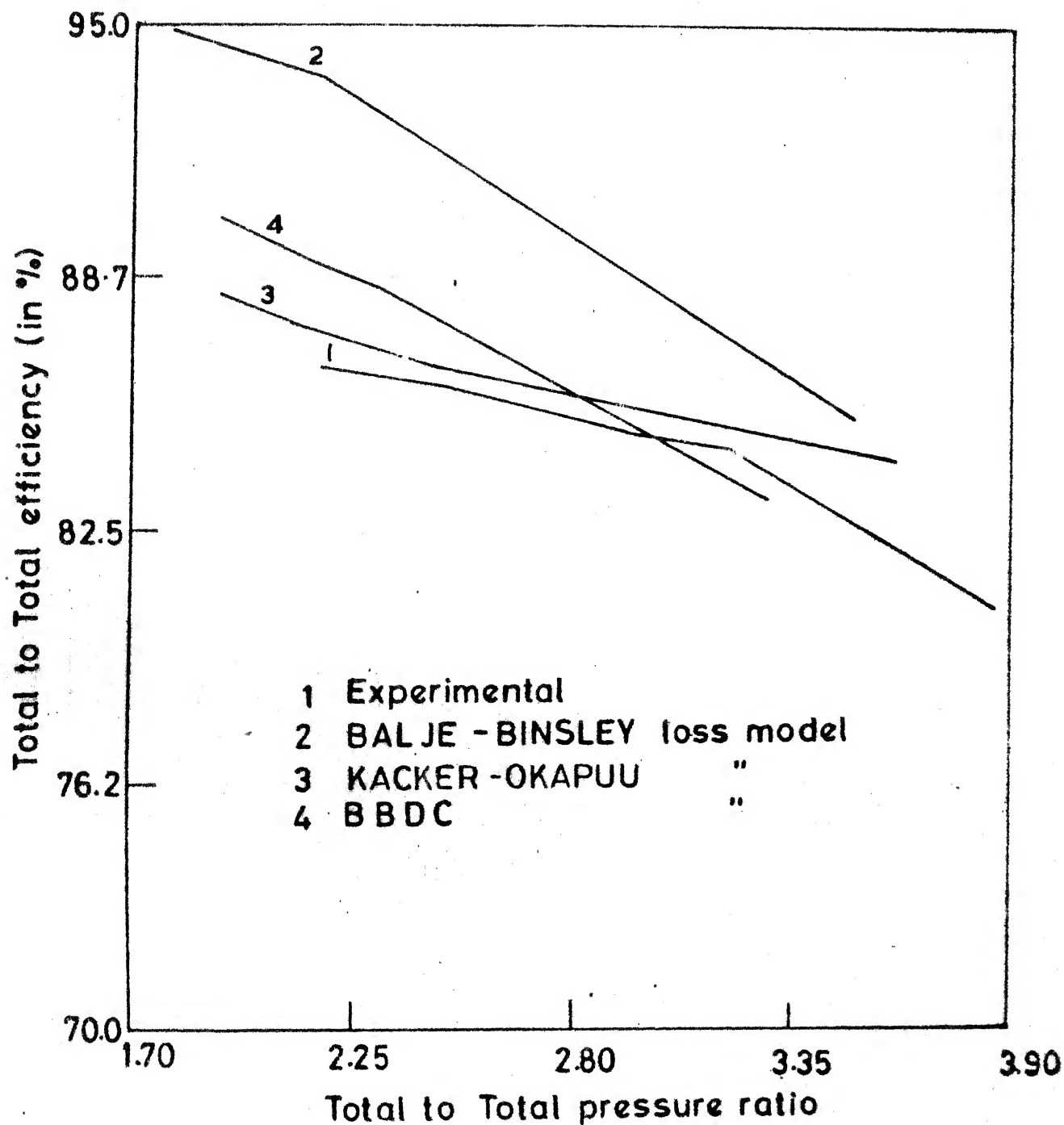
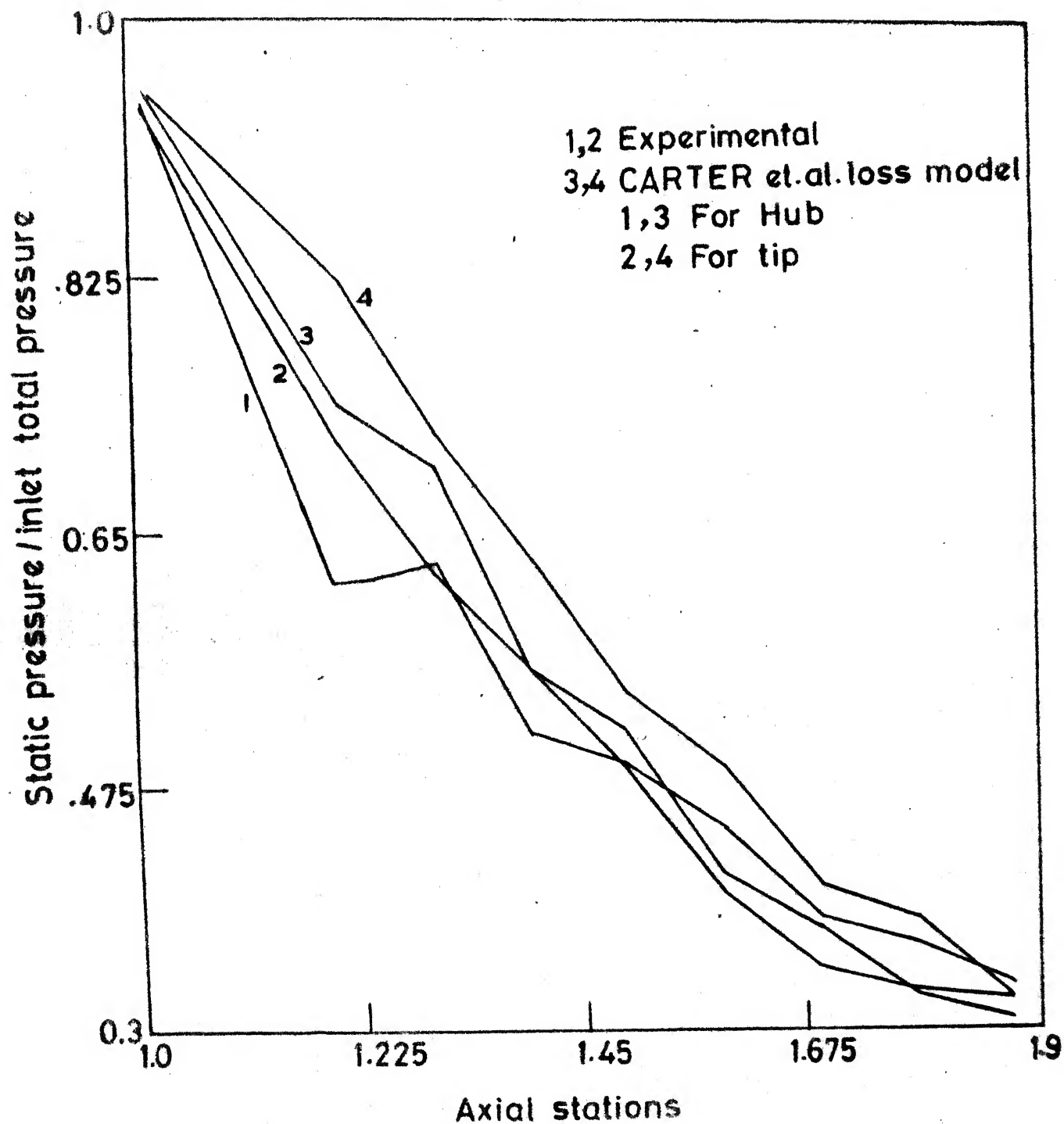FIG. 27 TOTAL TO TOTAL EFFICIENCY VS TOTAL PRESSURE RATIO FOR TEST CASE No. 3

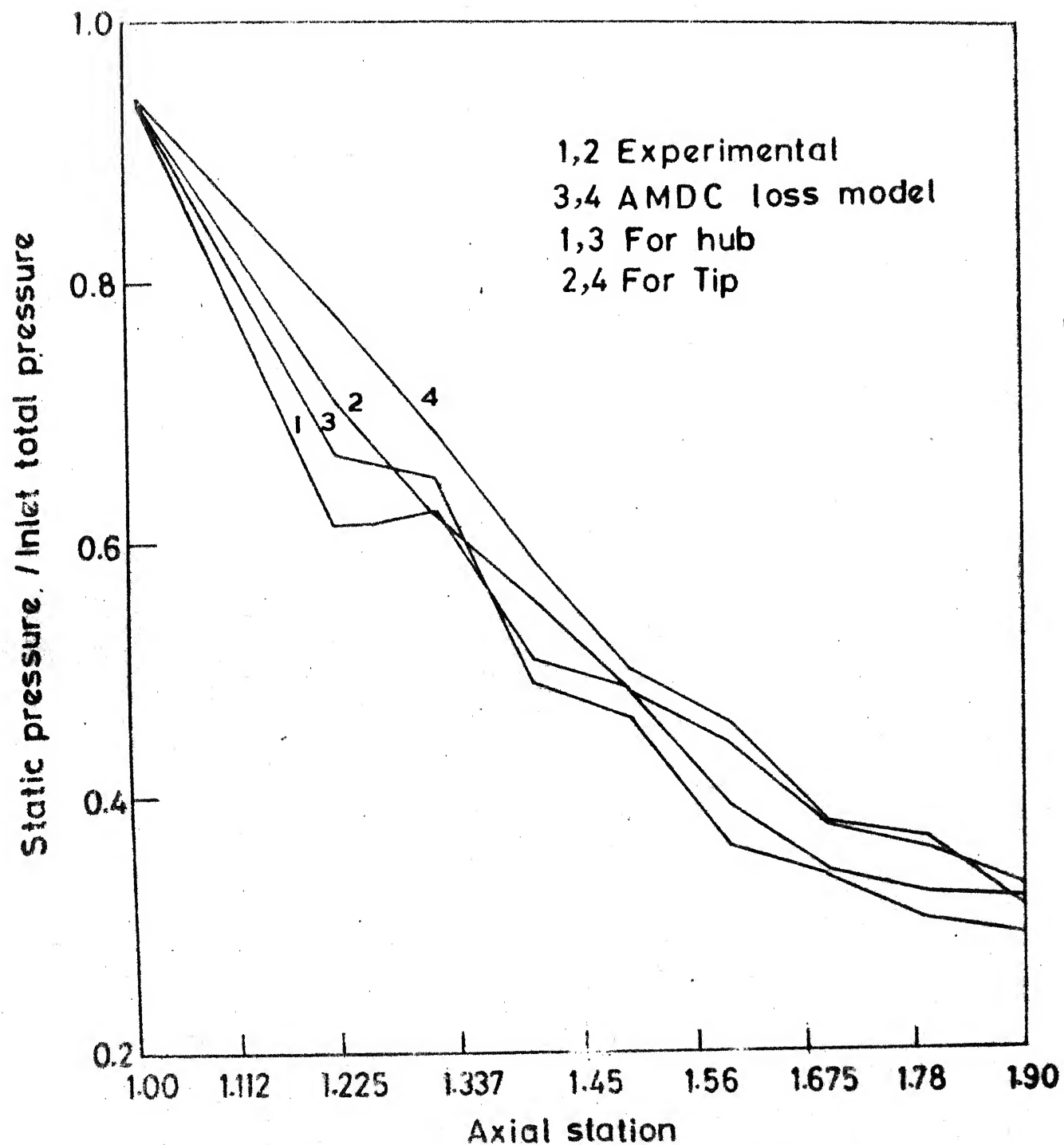FIG.28 HUB AND TIP STATIC PRESSURE DISTRIBUTION FOR TEST CASE No. 3

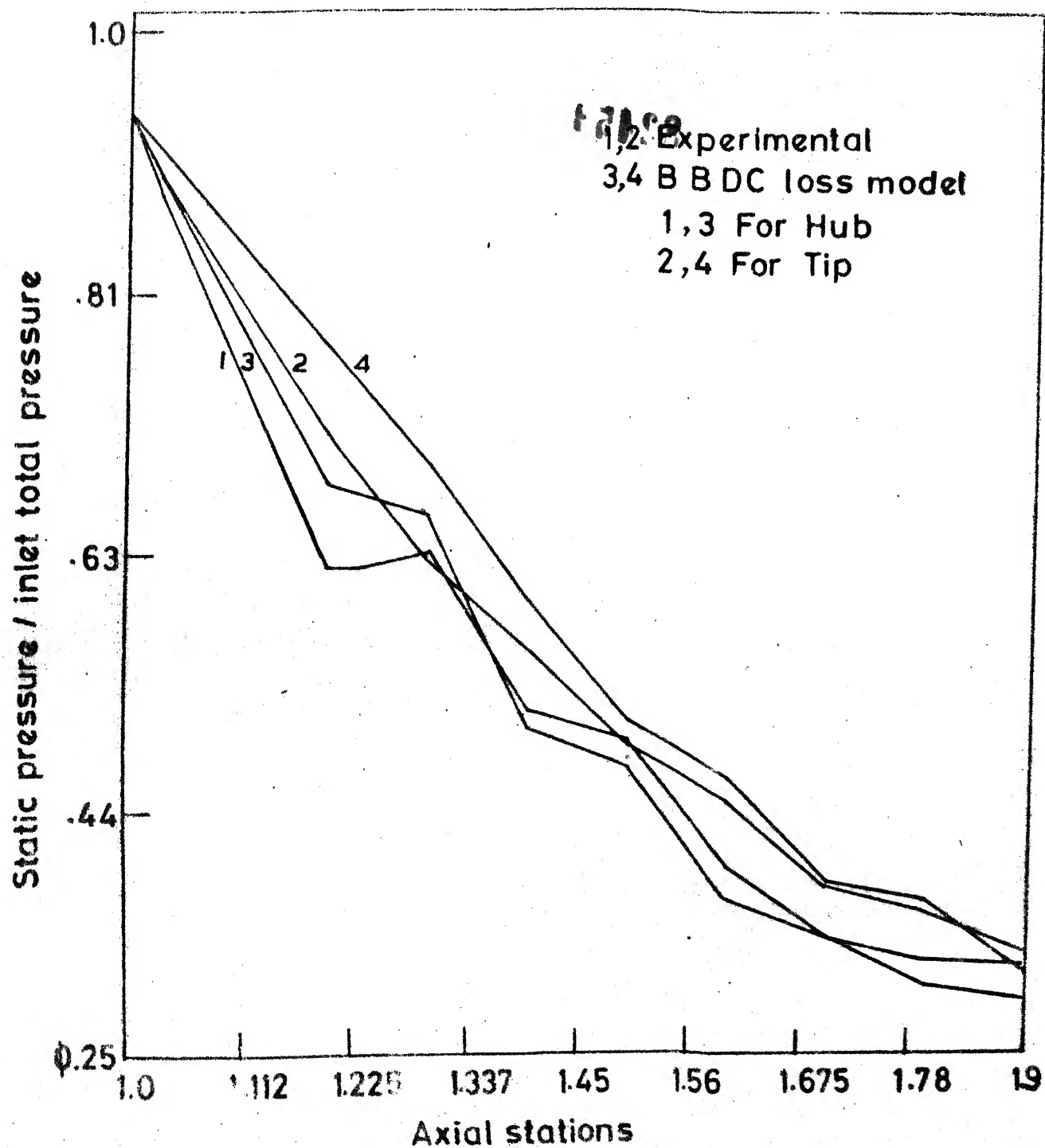FIG.29 HUB AND TIP STATIC PRESSURE DISTRIBUTION FOR TEST CASE No. 3

FIG.30 HUB AND TIP STATIC PRESSURE DISTRIBUTION
FOR TEST CASE No. 3